Evaluation of Neuroprotective Interventions in Different *Pde6a* Mutant Animal Models for Retinitis Pigmentosa

Inaugural-Dissertation

zur Erlangung des Doktorgrades der Medizin

der Medizinischen Fakultät

der Eberhard Karls Universität

zu Tübingen

vorgelegt von

Jiao, Kangwei

2015

Dekan: **Professor Dr. I. B. Autenrieth**

1. Berichterstatter: **Professor Dr. M. Ueffing**

2. Berichterstatter: **Professor Dr. R. Lukowski**

Abstract

Purpose. Retinitis Pigmentosa (RP) relates to a heterogeneous group of blinding diseases, which collectively affect about 1 in 4000 individuals worldwide. The large genetic diversity in the mutations causing RP, even when affecting the same gene, leads to very different degeneration phenotypes. Previously, research on *Pde6* mutant animals has focused on *Pde6b* mutants (Keeler 1924, Chang, Hawes et al. 2002). *Pde6a* mutants have been far less studied, although mutations in the *Pde6a* gene can also cause the death of rod photoreceptors and RP.

Methods. Our experiments were divided into two steps: Characterization of retinal degeneration in vivo, and treatment of *Pde6a* mutants in in vitro condition. With the characterization of retinal degeneration in vivo, we used different homozygous pde6a mutant mice. Namely, the *V685M*, *D670G*, *R562W*, and *V685M*R562W* variants. We used a variety of degeneration markers (*i.e.* TUNEL, Caspase-3, Calpain activity, PARP activity, PAR accumulation) to study the progression in photoreceptor degeneration of these *Pde6a* mutants at different post-natal (PN) days in vivo. With the treatment of *Pde6a* mutants in vitro condition, we used organotypic retinal explant cultures treated with the PARP specific inhibitor PJ34 to confirm the causal involvement of PARP activity in the neurodegenerative process.

Results. Our study indicated that the speed of retinal degeneration varied in the four *Pde6a* mutant situations ***in vivo*,** the progression of photoreceptor degeneration was always correlated in time with an excessive activation of Calpain and PARP, accumulation of PAR, positive reaction in the TUNEL assay, but activation of Caspase-3 was not detected. Organotypic retinal explant cultures treated ***in vitro*** with PJ34 showed a significant increase in the number of surviving photoreceptors in *V685M*R562W*, *R562W*, and *D670G* retinae. However, in the *V685M* mutant, there was no significant difference between both of groups.

Conclusion. We showed that Calpain, PARP, and PAR play a dominant role in the mechanism of photoreceptor degeneration in different Pde6a mutants. We highlight PARP as a common target for neuroprotective interventions in RP caused by *Pde6a* mutations. Furthermore, our study may serve to predict time-courses of retinal degeneration in human RP patients suffering from *Pde6a* mutations and could help to define the optimal time-points for clinical interventions.

Tables of contents

Abstract **3**

List of Tables **8**

Abbreviations **9**

1. Introduction **12**

1.1 Retinal structure and visual transmission in vertebrates 12

1.1.1 Overview of the vertebrate retina 12

1.1.2 Visual Transmission in vertebrate 14

1.2 Retinitis Pigmentosa. Disease Pathology and Genetics 15

1.2.1 Clinical presentation and histopathologic of retinitis pigmentosa 15

1.2.2 Genetics of retinitis pigmentosa 16

1.3 Phosphodiesterase (PDE) in retinal degeneration 17

1.4 Animal models for retinitis pigmentosa 18

1.4.1 Retinal degeneration models. Pde6a Mice 18

1.5 Calpain family 21

1.5.1 Calpain in neuronal and inherited retinal degeneration 22

1.5.2 Caspase-dependent apoptosis 23

1.5.3 Caspase-independent apoptosis 23

1.6.1The role of the PARP in retinal degeneration 25

1.7 Treatment strategy in retinitis pigmentosa 26

1.7.1 Background 26

1.7.2 Neuroprotection 26

1.7.3 Neuroprotection of Pde6a retinas using a specific inhibitor of PARP 27

1.8 Aims of study 28

2. Materials and methods 29

2.1 Materials 29

2.2 Methods 35

2.2.1 Animal procedures 35

2.2.2 Tissue Preparation (Embedding and section) 36

2.2.3 Dissection of retina 37

2.2.4 TUNEL (In Situ Cell Death Detection Kit) assay 37

2.2.5 Caspase 3 immunostaining 39

2.2.6 Calpain activity Assay 39

2.2.7 Poly ADP ribose polymerase In-situ Enzyme activity Assay (PARP) 40

2.2.8 Poly (ADP-ribose) (PAR) immunohistochemistry 41

2.2.9 Microscopy, cell counting, and statistical analysis 42

3. Results 44

3.1 Characterization of four *Pde6a* mutants *in vivo* 44

3.1.1 The peak of photoreceptor cell death in different Pde6a mutants in vivo 44

3.1.2 Cell death in Pde6a mutants 46

3.1.3 Calpain activity is increased in Pde6a mutants and wild type retina in vivo 46

3.1.4 PARP activity in Pde6a mutants in vivo 48

3.1.5 PARylated proteins in Pde6a mutants in vivo 48

3.1.6 Summary of characterization of Pde6a mutants in vivo 52

3.2. Treatment of *Pde6a* mutants *in vitro* 53

3.2.1 PARP inhibition delays photoreceptor cell death in Pde6a mutants in vitro 53

3.2.2 PARP inhibition positively affected photoreceptor survival in Pde6a mutants in vitro 54

3.2.3 PARP inhibition decreases Pde6a mutant PAR-positive cells in vitro 56

3.2.4 Summary of treatment results on four Pde6a mutants in vitro 58

4. Discussion 59

4.1 Hereditary retinal degeneration and photoreceptor cell death 59

4.2 Cell death mechanism in *Pde6a* mutants 60

4.3 The role of PARP in retinal degeneration 62

4.4 Conclusion 64

4.4.1 Alternative cell death routes involving Calpain and PARP 64

4.4.2 PARP as a therapeutic target in Pde6a retinitis pigmentosa 65

4.4.3 Perspectives for future treatment developments 65

5. Zusammenfassung 67

6. Publication or Presentations 68

7. Curriculum Vitae 69

8. Acknowledgements 70

9. Bibliography 72

Statement of Authorship 82

List of Figures

Figure 1. Cross-section of the retina 12
Figure 2.Photographs of a Retinitis pigmentosa retina 16
Figure 3.The V685M mice 19
Figure 4.The D670G mice 20
Figure 5.The R562W mice 20
Figure 6.The V685M*R562W mice 21
Figure 7.The multifaceted nature of PARP 24
Figure 8.Retinal explants cultures 35
Figure 9. TUNEL assay and cell death in Pde6a mutants 45
Figure 10.Activation of Calpain and Caspase-3 assay in Pde6a mutants 47
Figure 11. Differential regulation of markers linked to cell death in *Pde6a* mutants 50
Figure 12. PARP activity and PARylation accumulation in different *Pde6a* mutants 52
Figure 13. PARP inhibition in short-term cultures of *Pde6a* mutants 55
Figure 14. PARP inhibition in long-term cultures of *Pde6a* mutants 56
Figure 15. PARP inhibition decreases the number of PAR polymers in cells in the ONL in the different *Pde6a* mutants 57

List of Tables

Table 1.Animal models used in the study 19
Table 2.Materials and Products 29
Table 3.Antibodies used in immunohistochemistry 32
Table 4.Characterization of *Pde6a* mutants *in vivo* 53
Table 5.Treatment of four *Pde6a* mutants in vitro 58
Table 6.Gradient of different assays in *Pde6a* mutants in vivo 61

Abbreviations

µg	microgram
µl	micrometer
µM	micromolar
AAV	Adeno-associated virus
ADRP	Autosomal dominant retinitis pigmentosa
ADP	Adenosine diphosphate
AIF	Apoptosis inductor factor
AMD	Age-related macular degeneration
Apaf-1	Apoptosis activating factor-1
ARRP	Autosomal recessive retinitis pigmentosa
ARVO	Association for research in vision and ophthalmology
ATP	Adenosine rri-phosphate
BER	Base excision repair
cAMP	cyclic Adenosine Monophosphate
Ca^{2+}	Calcium
cGMP	cyclic guanosine-mono-phosphate
DAB	Di-amino benzidine
DAPI	4',6-diamidino-2-phenylindole
DMSO	Dimethylsulfoxide
DNA	Deoxyribose nucleic acid
ERG	Electroretinography
Fig.	Figure
GC	Guanylate cyclase

GCAP	Guanylate cyclase-activating protein
GDP	Guanosine diphosphate
GCL	Ganglion cell layer
GEF	Guanine effector protein
GK	Guanylate kinase
GMP	Guanosine monophosphate
GTP	Guanosine triphosphate
h	Hour
HRDs	Hereditary retinal disorders
INL	Inner nuclear layer
IPL	Inner plexiform layer
IS	Inner segment
KO	Knockout
Min	Minute
mRNA	Messenger RN
Na^+	Sodium
NAD^+	Nicotinamide adenine dinucleotide
NAM	Nicotinamide
ONL	Outer nuclear layer
OPL	Outer plexiform layer
OS	Outer segment
PN	Post-natal day
PAR	Poly aDP ribose
PARP	Poly aDP ribode polymerase
PBS	Phosphate buffered saline

PBST	Phosphate buffered saline with Triton or Tween
PCR	Polymerase chain reaction
Pde5	Phosphodiesterase 5
Pde6	Phosphodiesterase 6
Pde6α	Phosphodiesterase 6 α-subunit
Pde6β	Phosphodiesterase 6 β-subunit
Pde6γ	Phosphodiesterase 6 γ-subunit
$Pde6\alpha^{V685M}$	Phosphodiesterase 6 α-subunit V685M
$Pde6\alpha^{V685M*R562W}$	Phosphodiesterase 6 α-subunit V685M*R562W
$Pde6\alpha^{R562W}$	Phosphodiesterase 6 α-subunit R562W
$Pde6\alpha^{D670G}$	Phosphodiesterase 6 α-subunit D670G
PJ34	(N- (6-oxo-5, 6-dihydrophenanthridin-2-yl)-N, N dimethylacetamide. HCl)
PN	Post-natal day
P23H	Proline 23 histidine
rd1	Retinal degeneration 1
RP	Retinitis Pigmentosa
RPE	Retinal pigment epithelium
RT	Room temperature
S334ter	Serine 334 truncation
SD	Sprague dawley
TBS	Tris buffered saline
TUNEL	Terminal deoxynucleotidyl transferase dUTP nick end labelling
wt	Wild-type
XLRP	X-linked retinitis pigmentosa

1. Introduction

1.1 Retinal structure and visual transmission in vertebrates

1.1.1 Overview of the vertebrate retina

The anatomical structure of the vertebrate retina is comprised of 10 layers (The Retinal Tunic. Virginia-Maryland Regional College of Veterinary Medicine). These layers are : The retinal pigment epithelium (RPE), the photoreceptor layer (PL), the external limiting membrane (ELM), the outer nuclear layer (ONL), the outer plexiform layer (OPL), the inner nuclear layer (INL), the inner plexiform layer (IPL), the ganglion cell layer (GCL), the nerve fiber layer (NFL) and the inner limiting membrane (ILM).

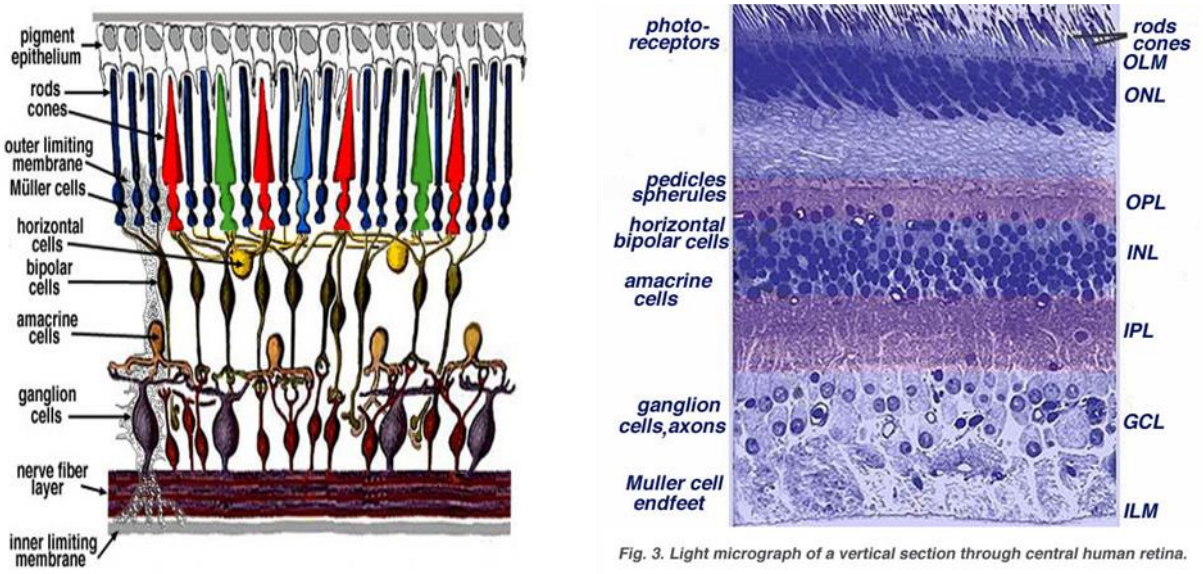

Figure 1. Cross-section of the retina

The photoreceptors (rods and cones) convert photons into neurochemical energy, which is relayed through the retina. The different layers of the retina process the image signal. The output of the retina comes from the retinal ganglion cells, whose axons gather at the optic disc to form the optic nerve. In retinitis pigmentosa and age-related macular degeneration, the photoreceptors are degenerated but the other layers of the retina remain functional. (Image is taken from www.webvision.med.utah.edu.)

The Inner limiting membrane (ILM) is essentially a base membrane, which is the innermost layer, and is formed by the end feet of Müller cells. Its function is to separate the retina from the vitreous. The Nerve fiber layer (NFL) is formed by the axons of ganglion cells, running between this layer and the ILM. It passes in parallel through the lamina cribrosa to form the optic nerve. The Ganglion cell layer (GCL) is formed by the somas of retinal ganglion cells whose axons form the optic nerve. It mainly contains two types of ganglion cells, the midget ganglion cells that are present in the macular region and polysynaptic ganglion, which lie predominantly in the peripheral retina.

The Inner plexiform layer (IPL) is a nerve fiber layer where the synapses between bipolar cells, amacrine cells, and ganglion cells are located. The Inner nuclear layer (INL) mainly consists of the nuclei of bipolar and amacrine cells, which are surrounded by capillaries in the central retina, and nuclei of avascular amacrine cells in the outer layer. The Outer plexiform layer (OPL) consists mainly of connections of rod spherules with the dendrites of bipolar cells, and cone pedicles with horizontal cells.

The Outer nuclear layer (ONL) consists of cells bodies of both rod and cone photoreceptors, which contain a photosensitive substance, rhodopsin, which participates in peripheral and scotopic vision: and cones; which also contain a photosensitive pigment and are primarily responsible for central and color vision. The External limiting membrane (ELM) is a fenestrated membrane that separates the inner segments of photoreceptors from their nucleus and allows both the rods and cones to maintain their structure through mechanical strength. The Retinal pigment epithelium (RPE) is the outermost layer of the retina, and consists of a single layer of cells containing the pigment melanin.

There are only 1.2 million optic nerves even though there are 130 million photoreceptor cells in the human retina. Vision is formed after light reaches the retina and the transduction of visual stimuli to electrical stimuli begins. This transduction of visual signals relies on the physiological state of each cell. There are two sorts of photoreceptor cells existing in the retina, rods and cones. Rods, which have higher sensitive to light but

fail to provide for highly discriminated central vision, and the cones which only account for 3% of total retinal photoreceptor cells (Szel and Rohlich 1992), and are mainly responsible for high discrimination in central vision, color vision and photopic vision. Signals of rod and cone cells take relatively independent positions in the transduction pathway of retina.

1.1.2 Visual Transmission in vertebrate

Visual photo-transduction is a process, which first takes light into the eye, then a biological conversion of that light transfers it into an electrical signal in the retina through the rhodopsin pathway. Subsequently, rhodopsin is rapidly decomposed into opsin and retinene. Opsin activates the protein transducin and binds GTP, and then the GTP-α complex activates phosphodiesterase (PDE). This leads to cGMP break down to 5'- GMP through the Na^+ pathway, as PDE hydrolyzes cGMP. Reduced levels of cGMP cause cyclic nucleotide gated channels to close preventing influx of Na^+ and Ca^{2+}. The extracellular influx of Ca^+ through L-type Ca^+ channels is the requirement for the photoreceptor cells to release glutamic acid. However, a L-type Ca^+ pathway gene mutation will lead to blindness (Schmitz and Witkovsky 1997)

Vision results from the decomposition of rhodopsin, a pigment molecule that is extremely sensitive to light. The cones pigment is a chemical substance of the outer segment membrane; it is similar to the rhodopsin in the rods, and is also responsible for color vision and contains the same chemical, retinene. Primates have three principal color receptors in their retina. These three types of cones are sensitive for light at different wave-lengths; short-wavelength (S-cones 440nm) sensitive, or blue light, middle-wave-length (M-cones 545nm) sensitive for green light and long-wavelength (L-cones 565nm) sensitive for red light, respectively. Perception of color can be synthesized by these three principal color receptors for individual colors. Though coded by these three different colors, the human eye is able to perceive a wide range of colors. While the greatest difference between cone and rod cells is the mechanism for photoelectric conversion that they employ, cone bipolar cells also make synaptic connections with the dendrites of ganglion cells without passing through the loop of an amacrine cell, as in the rod pathway. Consequently, the cone pathway features

advantageous characteristics such as being more direct and having a smaller convergence.

There are several varieties of proteins participating in photoelectric conversion, the accurate functions of some of which are still not unknown. In the case of changes in the structure and function of photoreceptor cells and their internal signaling molecules due to gene mutation and environmental damage, the photoreceptor cells function will become abnormal and even incurs apoptosis. It is important to indicate that any abnormality in quality and quantity of any molecule will influence the light transduction process. The pathological change of retinal pigment degeneration results from the dysfunction of the rod cells.

1.2 Retinitis Pigmentosa. Disease Pathology and Genetics

1.2.1 Clinical presentation and histopathologic of retinitis pigmentosa

Retinitis Pigmentosa (RP) is a hereditary neurodegenerative disease of the retina, which affects photoreceptors and is a major cause of early-onset blindness in the industrialized world. In the clinic, the fundus of Retinitis pigmentosa patients include attenuated vasculature, intraretinal pigmentary deposits and bone spicules. When pale optic disc symptoms emerge, it usually means the patient is often already in an advanced disease stage. Retinal pigmentation, attenuated vasculature, together with the pale optic disc, made up what is called the RP triad.

In typical cases, the retinal pigment degeneration first affects rods. Due to the abnormal toxic effect of proteins or due to abnormal enzymatic activity, the rod outer segments (OS) are reduced and gradually shortened; the internal structure of OS is reshaped, followed by opsin rearranged to the inner segment (IS); and finally the axon retreats from the synaptic connections in the OPL. Eventually, the cones will suffer from secondary death (Marc, Jones et al. 2007). Photoreceptor cell degeneration mainly presents from the perspective of tissue pathology, the outer nuclear layer will become thin and disappear and the outer plexiform layer and other relevant tissues and cells of the retina will change secondarily. Clinically, pathogenic locations are generally seen at the equator of the retina, which corresponds to the distribution of rods in the retina.

There are very few rod cells in the fovea of the retina, however, their density reaches a maximum at 20° from the center and is gradually reduced outwards. Therefore, the disease is often characterized by a ring scotoma. However, cone cells incur secondary death after the degeneration of rod cells in hereditary retinal pigment degeneration, which may be associated with the oxidative damage and interaction of cone and rod cells (Mohand-Said, Hicks et al. 2000, Ying, Jansen et al. 2000, Yu and Cringle 2005).

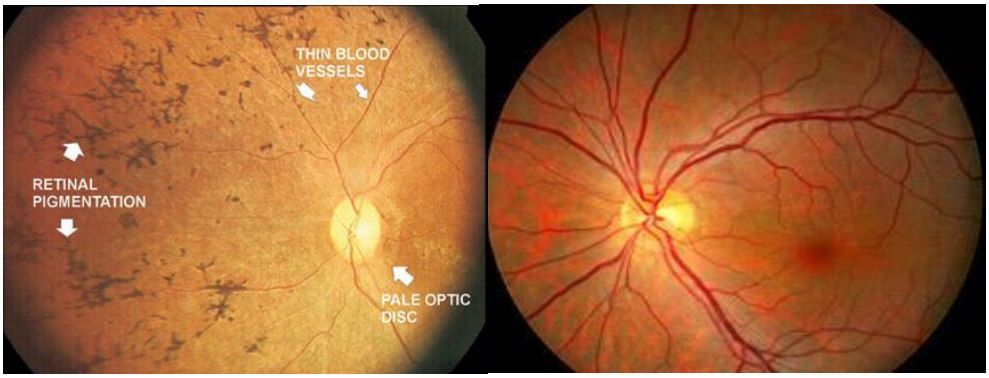

Figure 2.Photographs of a Retinitis pigmentosa retina

Photographs of the retinitis pigmentosa retina (left) and normal (right). Typical RP features are evident in the affected retina (upper left) including marked pigment epithelial thinning, retinal vascular attenuation, classical 'bone spicule' and intraretinal pigmentary deposits (Image taken from: www.rpfightingblindness.org.uk/index.php?tln=aboutrp&pageid=71).

1.2.2 Genetics of retinitis pigmentosa

Retinal pigmentosa refers to a highly hereditary heterogeneous disease, which is characterized by degeneration due to rod photoreceptor cell damage. The retina suffers from internal damage and neuroglia hyperplasia and finally severe visual dysfunction is presented due to the cone photoreceptor cell death (Fariss, Li et al. 2000, Hartong, Berson et al. 2006). The disease is divided into autosomal recessive (AR), approximately 50-60%; autosomal dominant (AD), about 30-40%; and dominant X-linked (XL) hereditary, around 5-15% (Hartong, Berson et al. 2006, Chizzolini, Galan et al. 2011). There are over 67 known RP causative genes (https://sph.uth.edu/retnet/sumdis.htm),

of which 23 are autosomal dominant hereditary genes, 41 are autosomal recessive hereditary genes and 3 are dominant X-linked genes, of which *Pde6a* is an autosomal dominant. A study conducted an SSCP analysis of 22 exons of 164 irrelevant patients *Pde6a* gene and a sequence testing of abnormal variants. They found 8 different mutant diseases in 6 ARRP families, of which 2 are nonsense mutations and 5 are missense mutations. One mutation influences the classic splice donor site, thus 3-4% of ARRP patients in North America are affected by the *Pde6a* gene mutation (Dryja, Rucinski et al. 1999).

1.3 Phosphodiesterase (PDE) in retinal degeneration

Phosphodiesterase (PDE's) regulates the levels of the signaling molecule cAMP (guanylate cyclase-activating protein) and cGMP (cyclic guanosine monophosphate). In photoreceptors, PDE6 hydrolyses cGMP, which is the key signaling molecule in the vertebrate photo-transduction cascade. According to the different forms of the protein, PDE6 could be divided into rod-PDE6 and cone-PDE6. Retinal rod cell holoenzyme refers to a tetramer composite, consisting of two larger catalytic subunits (α and β) and two smaller regulatory subunits (γ), respectively encoded by *Pde6a*, *Pde6b, Pde6g* genes. All mutations occurring in any of the three *PDE6* subunits together may be responsible for up to 10% of human RP patients (Bayes, Giordano et al. 1995, Tsang, Gouras et al. 1996, Dryja, Rucinski et al. 1999).

cGMP is an essential target for phosphodiesterase in the vertebrate retina and its contribution to sensitivity regulation in rods (Koutalos, Nakatani et al. 1995). Photoexcitation in vertebrate rod photoreceptor cells occurs through a light-activated cGMP enzyme cascade. Absorption of a photon by the receptor molecule rhodopsin, leads to the activation of a potential cGMP phosphodiesterase, which rapidly hydrolyzes cytosolic cGMP. The transient decrease of cGMP concentration causes the closure of the cGMP-sensitive channels on the plasma membrane and results in hyperpolarization of the cell (Fesenko, Kolesnikov et al. 1985, Liebman 1987). Its dynamic concentration is made of hydrolysis of *Pde6a* (Phosphodiesterase 6a-subunit) and cGMP, which is a key subunit for transducin, and the process of participating in visual signal transduction.

Pde6-a gene mutation has already been confirmed as one of the factors causing autosomal recessive retinal inflammation (provided by RefSeq, Jul. 2008).

1.4 Animal models for retinitis pigmentosa

Hereditary retinal degenerations are a group of blinding eye diseases with the progressive loss of photoreceptor cells indicated as its main characteristic. Though many disease-causing genes have already been confirmed, the mechanism of the photoreceptor death caused by gene defect still remains unknown. Therefore, there is no effective therapy at present. Further, it is hard to collect materials for retinal degeneration of human genetics (especially RP), so research mainly relies on animal models to probe its pathological process and pathogenesis. Previously, PDE6 dysfunction was investigated primarily on animal models affected by mutations in the *Pde6b* gene, such as the *rd1* (Keeler 1924) or the *rd10* mouse (Chang, Hawes et al. 2002). A variety of *Pde6a* mutations are also known to cause RP (Sakamoto, McCluskey et al. 2009), but so far these have been relatively little studied.

1.4.1 Retinal degeneration models. Pde6a Mice

The *Pde6a* mice carry a loss-of-function mutation in the gene for the alpha-subunit of the rod photoreceptor cGMP phosphodiesterase 6 (*Pde6-a*). Different *Pde6a* mutations in the animal may contribute to the differences in the mechanisms in rods and cones in various ways. Here, we used four different animal models to try to understand photoreceptor cell death mechanisms. All *Pde6a* mutants used were of the C57BI6/J strain. Three out of four models with *Pde6a* mutations, homozygous D670 and V685, have been identified in a G3 ethyl nitrosourea (ENU) mutagenesis screen, and generated a new mouse model for the R562W mutation. The original residues mutated in these *Pde6a* models encode for amino acids that are highly conserved across species both at the nucleotide and amino acid level. Mice with abnormal fundus pigmentation were observed by indirect ophthalmoscopy in a colony of ENU mutagenized G3 A.B6-Tyr^{+}/J mice in the Neuroscience Mutagenesis Facility (NMF) at The Jackson Laboratory. Based on the homozygous mutants, we then generated compound heterozygous *Pde6a*^{V685M*R562W}. The homozygous *Pde6a*^{R562W}, which reproduces the human blinding

disease retinitis pigmentosa, was obtained from the company *GenOway* (Sakamoto, McCluskey et al. 2009).

Table 1.Animal models used in the study

Official Line Designation	Genetic defect	Source
V685M	mutation in alpha-subunit of the rod photoreceptor cGMP phosphodiesterase 6	Jackson Laboratory
*V685M*R562W*		Tübingen university
R562W		GenOway
D670G		Jackson Laboratory
C57BI6/J	Wild type	Jackson Laboratory

Figure 3.The V685M mice

The V685M mice were obtained from Jackson Labs (Bar Harbor, MA, USA) (Stock No. 006026). *Pde6a*^{V685M} and have been identified by the fine structure map containing 12 genes, according to the Ensembl database (http://www.ensembl.org), including *Pde6a*, an excellent candidate gene. Sequencing of both *Pde6a* cDNA and genomic DNA from A.B6-Tyrþ/J-*Pde6a*$^{nmf282/nmf282}$ mice revealed a single nucleotide G to A missense mutation in exon 16, which is predicted to cause an amino acid change from valine to methionine (V685M). The valine residue is highly conserved among zebrafish, mouse, dog, human and bovine, suggesting its importance in the catalytic function of *Pde6a* (Sakamoto, McCluskey et al. 2009).

Figure 4.The D670G mice

The cDNA and genomic DNA of D670G were from *C57BL/6J Pde6a*$^{nmf363/nmf363}$ mice and were directly sequenced for altered fundus pigmentation (Sakamoto, McCluskey et al. 2009). ENU mutagenesis was used to create an A to G transition that results in an amino acid substitution of glycine for aspartic acid at position 670 (D670G) in *Pde6a*. This *Pde6*^{anmf363} mutation, is located in the catalytic domain of *Pde6a,* and is 15 amino acids away from the *Pde6a*^{nmf282} mutation. The aspartic acid residue at position 670 is also highly conserved among zebrafish, mouse, and dog, human and bovine (Sakamoto, McCluskey et al. 2009). *Pde6a*^{D670G} mice were provided by Jackson Labs (Bar Harbor, MA, USA) (MGI ID: 3828520).

Despite the fact that these mutations are located within the catalytic domain of the *Pde6a* protein, the biochemical consequences of the mutations differ (Sakamoto, McCluskey et al. 2009). The valine 685 residues in *Pde6a*^{V685M} are more important than *Pde6a*^{D670G}.

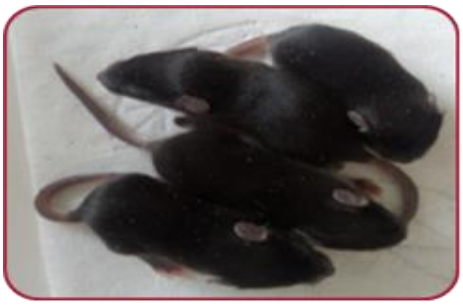

Figure 5.The R562W mice

The R562W knock-in mutant was generated by *Genoway* (Lyon, France). The generation of this mutant followed the identification of a human RP patient with compound

heterozygous for the c.1684C>T/p. Arg562Trp and c.2053G>A/p. Val685Met mutations in *Pde6a*.

To identify the homozygous *Pde6a*^{R562W} animals, the progeny resulting from the F2 breeding mice was screened using a PCR specific for the wild-type *Pde6a* allele. For the detection of the point mutant Knock-in allele, the primer set 87213oth-PDF1/87214oth-PDF1 was designed flanking the remaining *lox*P site.

Figure 6.The V685M*R562W mice

RP animal models are normally studied in the homozygous state, even though in human RP patients, homozygosity is relatively rare and, in fact, compound heterozygosity, where two different disease causing alleles come together in one individual, is more common. Therefore, crossbreeding of the *Pde6a*^{R562W} knock-in with the *Pde6a*^{V685M} mutant, gave the opportunity to recreate and study an actual patient genotype. This animal model is exactly homologous to a human RP patient genotype and represents one of the first ever attempts to create a patient matched animal model for the development and assessment of an individualized therapy for RP. The generation of this mutant followed the identification of a human RP patient who was compound heterozygous for the e.1684C>T/p. Arg562Trp and e.2053G>A/p.

1.5 Calpain family

It was officially named Calpain or calcium activated neutral protease (CANP) in 1991 (Guroff 1964), and was first isolated and purified in the skeletal muscle of the chicken in 1978 (Ishiura, Murofushi et al. 1978). The cDNA of the enzyme was first cloned in 1984 (Ohno, Emori et al. 1984). Calpain is a type of non-soluble restriction proteolytic enzyme that exists in almost all mammalian cells. It belongs to a family of at least 16 members of

calcium-dependent cysteine proteases (Huang and Wang 2001). In mammals, the two major isoforms, Calpain1 (μ-Calpain) (Kishimoto, Kajikawa et al. 1981) and Calpain2 (m-Calpain) (Dayton, Goll et al. 1976) are activated by micro molar and millimolar Ca^{2+} concentrations, respectively. According to their histological distribution, the Calpain family is divided into two categories. Specific Calpains includes Calpain3 (skeletal muscle), Calpain8 (smooth muscle), Calpain9 (stomach), and non-specific Calpains, such as Calpain1, 2, 10 etc. The physiological role of Calpain is still poorly understood, but they have been shown to be active participants in processes of cell mobility and cell cycle progression (Hood, Brooks et al. 2006).

1.5.1 Calpain in neuronal and inherited retinal degeneration

Calpain as a calcium-binding protein has been shown to have a direct correlation with cell death. In certain conditions, when the concentration of intracellular Ca^{2+} is increased (Azarian, Schlamp et al. 1993, Gressner, Lahme et al. 1997), it can cause Ca^{2+} overload in mitochondria, activate the mitochondrial Calpain and trigger the cell death (Kar, Samanta et al. 2010). Na^{+}/Ca^{+} exchanger (NCX) is the main channel for the mitochondrial calcium clearance, along with the inducement of the death of smooth muscle cells (Kar, Chakraborti et al. 2009). Another pathway of cell death is dependent on Apoptosis-Inducing Factors (AIF), which are released from the mitochondrial membrane; apoptotic signaling can be divided into Caspase-dependent and Caspase-independent pathways. Apoptotic protein Cyt-C, apoptosis protease activating factor-1 (APAF-1), and procaspase 9 activate Caspase 9 and trigger downstream Caspase events, which constitute the route of classic mitochondrial apoptosis (Marek 2013).

Calpain plays an important role in intracellular signaling and calcium-induced neuronal degeneration as a calcium dependent cytosolic protease (Saito, Elce et al. 1993). The main cause of the RP disease is the specific expression of a gene mutation in the photoreceptor cells, and studies have shown that the ultimate way is apoptosis (Papermaster and Windle 1995). It is an important key in prevention and treatment of RP to understand how the genetic mutations produce and affect the factors, which induce the cell death of retinal cells. Calpain is directly correlated with cell death as a Ca^{2+} -binding protein. When Ca^{2+} concentration is elevated, the combination of Calpain

and Ca^{2+} activate the Calpain and participate and promote the apoptosis. The elevated level of the Ca^{2+} has been shown to be proportional to cell death as well as non-inherited models of RP (McConkey, Nicotera et al. 1989, Azarian, Schlamp et al. 1993, Gressner, Lahme et al. 1997). Ca^{2+} dependent Calpain-type proteases are ubiquitously expressed and are involved in neurodegeneration, including the retina and is usually associated with alternative non-apoptotic cell death mechanisms (Paquet-Durand, Azadi et al. 2006, Paquet-Durand, Sanges et al. 2010). Numerous studies have shown that Calpain activity is increased in many animal models for retinal degeneration including *Balb*/c mice, *rd*, *WBN/Kob* rats, *rd1*, *rd10*, *nmf137* (Donovan and Cotter 2002, Doonan, Donovan et al. 2003, Azuma, Sakamoto-Mizutani et al. 2004, Paquet-Durand, Azadi et al. 2006). The localization of Calpain activity is of major importance both for our understanding of the degenerative mechanisms and the assessment of potential neuroprotective treatments (Paquet-Durand, Silva et al. 2007). However, what part does Calpain play in retinal photoreceptor degeneration in *Pde6a* mutants, which have not been described previously?

1.5.2 Caspase-dependent apoptosis

Apoptosis is an extremely complex process, which requires a variety of factors to occur, such as pro-apoptotic factors and anti-apoptosis factors that eventually lead to apoptosis through a variety of ways. Calpain may interact with Caspases in a direct or indirect way, depending on the tissue specificity and difference in conditions. They have many common substrates. Enhancing the activity of Caspase-3 may reduce the intracellular level of Calpastatin that can indirectly promote the Calpain activation. Calpain can further cleave and prevent the activation of caspases (Nelson, Smuder et al. 2012). In the apoptosis of neuronal cells, Calpain cleaves and deactivates Caspases, but the activation can also be blocked by Calpain inhibition (Martinez, Zhang et al. 2010, Boehmerle and Endres 2011).

1.5.3 Caspase-independent apoptosis

Cells which are initially stimulated by apoptotic factors may see their intracellular Ca^{+} levels rise causing the activation of mitochondrial μ-Calpain. This cleaves AIF (Apoptosis-Inducing Factor) (62ku), which is a Caspase-independent death effector.

Afterward, the cells generate tAIF (57ku) and are detached from the inner mitochondrial membrane into the gap between the membranes, which can cause chromosome condensation and DNA degradation, finally leading to cell apoptosis (Chen, Paillard et al. 2011). Calpains may be the most important enzymes during the process of cleaving and releasing (Norberg, Orrenius et al. 2010). Therefore, to understand the function of mitochondrial Calpain in the regulation of cell apoptosis can not only contribute to the understanding of the molecular mechanisms of cell death, but may also provide new ideas for the development of drugs to eliminate Ca^{2+} overload and use selective Calpain inhibitors for the treatment of neurodegenerative diseases.

1.6 Poly-ADP-Ribose Polymerase (PARP) family

Poly-ADP-Ribose Polymerase (PARP) is a highly conserved nuclear enzyme in the eukaryotic cell. The PARP family is composed at least 18 different enzymes and plays an important role in DNA repair, replication, genome stability, regulation of cell proliferation and differentiation (Herceg and Wang 2001).

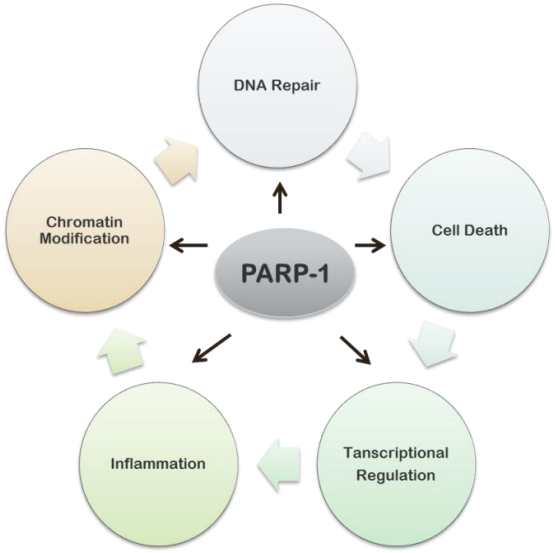

Figure 7.The multifaceted nature of PARP

Schematic delineation of the multifaceted nature of Poly (ADP) Ribose Polymerase (PARP), which include DNA repair, Chromatin Modification, Inflammation, Transcriptional Regulation, and Cell Death. Figure adapted from (Swindall, Stanley et al. 2013).

PARP-1 is one member of the PARP family (Malanga and Althaus 2005) and is a nuclear enzyme present in the nucleus, which is responsible for DNA repair and protein modification. PARP-1 contains a DNA-Binding domain, an auto-modification domain and a C-terminal catalytic domain. The relative molecular weight of that is 116,000 Dalton. Nuclear DNA damage and DNA breaks can lead to excessive PARP activation, which causes excessive NAD^+ utilization (nicotine amide adenine dinucleotide). Therefore, ATP (adenosine-5'-triphosphate) levels become depleted, leading to an energetic collapse and finally cell death. PARP is a critical factor during the cell death that involves accumulation of PAR (poly-ADP-ribose) and nuclear translocation of AIF (apoptosis inducing factor) from mitochondria. Excessive production of PAR by PARP-1 in response to extensive DNA damage may facilitate activation of different proteins, including DNA polymerases, topoisomerases, and transcription factors. PARP1 itself can also be down regulated by transfer ADP- ribose units from NAD^+, thus participating in the mechanism of DNA repair (Petrucco and Percudani 2008, Langelier, Planck et al. 2012).

Previous studies showed that the over activation of PARP may not only help to repair DNA damage, but could also cause further damage by reducing DNA stability and causing inflammation due to energetic collapse (Swindall, Stanley et al. 2013), In addition, excessive PARP-1 activation may also cause cell death independent of energy collapse due to a toxic level of PAR. Numerous studies showed that excessive PARP activation in the nucleus constitutes a nuclear signal that reaches to mitochondria (Berger, Sims et al. 1983), one route to cell death through PARP mediation may cause mitochondrial membrane depolarization and open the MPTP (mitochondrial permeability transition pores) (Sims, Berger et al. 1983, Du, Zhang et al. 2003), and finally cause DNA damage (Wang, Dawson et al. 2009). These studies indicated PARP as an important therapeutic target for the nervous system and other diseases associated with energy failure, for instance, RP. Therefore, further investigation is needed in more animal models, for example in *Pde6a* mutants.

1.6.1The role of the PARP in retinal degeneration

PARP plays a double role of DNA repair and protection of cells from toxic effects (Dantzer, Ame et al. 2006). Excessive activation of PARP not only plays an important

role in many neurodegenerative diseases (Wang, Dawson et al. 2009), it has also been proven to be involved in the cell death of retinal photoreceptors in retinal degeneration models (*rd1* mice*, P23H andS334ter* rats) (Paquet-Durand, Silva et al. 2007, Kaur, Mencl et al. 2011). Currently, oxidative stress is also considered to play an important role in hereditary retinopathy (Komeima, Rogers et al. 2007). An oxidative in particular DNA damage can lead to PARP activation. Excessive activation of PARP and high levels of PAR as a neurotoxin can lead to the cell death of neurodegenerative diseases (Yu, Kuncewicz et al. 2006, Vosler, Sun et al. 2009), in which PARP plays a leading role in the Caspase-independent apoptosis.

1.7 Treatment strategy in retinitis pigmentosa

1.7.1 Background

The treatment strategies of HRDs now focus on a variety of different approaches including stem cell transplantation, sub-retinal prosthetic devices, gene therapy, and neuroprotection. Each of these approaches is adequate only at a specific time-point with the progression of retinal degeneration. The main disadvantage of corrective gene therapy is its narrow applicability due to its limitation to only one gene/mutation, and the need to intervene as early as possible. Cell transplantation and prosthesis are applicable only once the degeneration has destroyed most or all of the outer retina, while neuroprotection is most useful at intermediate stages of HRD (Silverman and Hughes 1990, Lavail, Li et al. 1992, Aramant and Seiler 2004, Delyfer, Leveillard et al. 2004, Inoue, Iriyama et al. 2007).

1.7.2 Neuroprotection

Neuroprotection intends to improve neuronal survival in neurodegenerative diseases by strengthening neuronal metabolism using neurotrophic factors such as nerve growth factor (NGF), and blocking or delaying neuronal cell death mechanisms, using, for instance anti-apoptotic compounds (Bennett, Zeng et al. 1998, Uteza, Rouillot et al. 1999, Liang, Allen et al. 2000). Compared to gene therapy, neuroprotection is a mutation-independent approach that also benefits from a larger window-of opportunity, from the onset of HRD until almost the end of the degeneration (Trifunovic, Sahaboglu et al. 2012).

1.7.3 Neuroprotection of Pde6a retinas using a specific inhibitor of PARP

Previously, research on *Pde6* mutant animals has focused on *Pde6b* mutants, namely the *rd1* and *rd10* mouse models (Keeler 1924, Chang, Hawes et al. 2002). In these *Pde6b* mutants the activity of Poly (ADP-ribose) polymerase (PARP) was shown to be of major importance for the progression of photoreceptor degeneration (Paquet-Durand, Silva et al. 2007, Arango-Gonzalez, Trifunovic et al. 2014). To date, *Pde6a* mutants have been far less studied and here, we used two different homozygous *Pde6a* mutant mice, the *Pde6a*^{V685M*V685M} and the *Pde6a*^{R562W*R562W} animals. In the human situation homozygosity for a mutant allele is extremely rare, however, recently a small subgroup of RP patients was identified that carries a compound heterozygous *Pde6a*^{V685M}*R562W mutation. Therefore, we crossed *Pde6a*^{V685M*V685M} and *Pde6a*^{R562W*R562W} animals with each other to create a compound heterozygous *Pde6a*^{V685M*R562W} RP mouse model that was genotype-matched to human RP patients. Considering the above, Calpain and PARP activation played an important factor in photoreceptor degeneration of *Pde6a* mutants *in vivo*, therefore, targeting them by drug approaches may address a wide spectrum of RP mutations while working on a mutation independent neuroprotective therapeutic strategy. So, the aim is to investigate the efficacy of specific PARP inhibitors and explore the therapeutic potential in the neuroprotection of the degenerating retina by using the organotypic retinal culture protocol for *Pde6a*^{V685M} *Pde6a*^{V685M*R562W} *Pde6a*^{R562W} and *Pde6a*^{D670G} mice.

1.8 Aims of study

Nowadays, clinical patient care and the availability of integrated diagnostics for HRDs are not well established and most importantly, there is currently no effective cure available. Previous studies have shown an important role for Calpain and PARP activity in retinal degeneration in *rd1, rd10, P23H, S334ter* animal models (Sahaboglu, Tanimoto et al. 2010, Kaur, Mencl et al. 2011, Trifunovic, Sahaboglu et al. 2012). However, there are no studies about the potential involvement of PARP, PAR, Calpain and Caspase in *Pde6a* animal models for retinal degeneration.

Hence my work focused on the following aims:

1. Quantify photoreceptors undergoing cell death with TUNEL staining in *Pde6a*^{V685M}, *Pde6a*^{V685M*R562W}, *Pde6a*^{R562W} and *Pde6a*^{D670G} animal mutants *in vivo*
2. Measure the photoreceptor rows in *Pde6a* mutants at different time points *in vivo*
3. Study PARP and Calpain activity in photoreceptor degeneration in *Pde6a* mutants *in vivo*
4. Evaluate the neuroprotective potential of specific inhibitors on *Pde6a* mutant *retina in vitro.*

2. Materials and methods

2.1 Materials

Table 2.Materials and Products

Chemicals, Material, Devices, and software	Company	Product No.
Axio Imager Z1 Apo Tope Microscope	Carl Zeiss Micro Imaging GmbH, Gottingen	-
Axio Vision 4.7 Software	Carl Zeiss Micro Imaging GmbH, Gottingen	-
Caspase 3	Cell Signaling Technology, USA	P42574
Paraformaldehyde (PFA)	Sigma-Aldrich Chemie GmbH, Taufkirchen, Germany	P 6148
Pde6a ^{V685M} **B6.A Tyr^{+}-nmf282/J**	Jackson Labs	-
Pde6a ^{V685M*R562W}	Jackson Labs	-
Pde6a ^{R562W}	GenOway	-
Pde6a ^{D670G}	Jackson Labs	
C3H	Tübingen university	-
Adobe CS5 Design Standard Version12.0.3*32	Adobe systems GmbH, Munich, Germany	-
Culture Plate insert (only culture); 30mm Diameter, 0. 45µm pore sizes	Merck Millipore Ltd; Mill cell, Germany	PIHA 01250
Proteinase K	Sigma-Aldrich Chemie GmbH, Taufkirchen, Germany	P 6556
R16 Powder Medium (Basal)	Invitrogen Life Technologies, Darmstadt, Germany	07490743
Ethanol	Merck, Darmstadt, Germany	ETO-500-99-1

DAPI	Vector, Burlingame, CA, USA	D-9542
Dithiothreitol (DTT)	Sigma-Aldrich Chemie GmbH, Taufkirchen, Germany	43817
O.C.T™ Compound	Tissue-Tek, Leica, Bensheim, Germany	1418901035
Vectashield® DAPI	Vector, Burlingame, CA, USA	H-1500
Vectashield® without DAPI	Vector, Burlingame, CA, USA	H-1000
Diaminobenzidine (DAB)	Sigma-Aldrich Chemie GmbH, Taufkirchen, Germany	D5637
GraphPad Software Prism 6.01	GraphPad Software, La Jolla, CA, USA	-
BSA	Sigma-Aldrich Chemie GmbH, Taufkirchen, Germany	
Transferrin	Sigma-Aldrich Chemie GmbH, Taufkirchen, Germany	T-8027
Progesterone	Sigma-Aldrich Chemie GmbH, Taufkirchen, Germany	P-8783
Insulin	Sigma-Aldrich Chemie GmbH, Taufkirchen, Germany	I-6634
T3	Sigma-Aldrich Chemie GmbH, Taufkirchen, Germany	T6397-100mg
Corticosterone	Sigma-Aldrich Chemie GmbH, Taufkirchen, Germany	862290
Thiamine HCl	Sigma-Aldrich Chemie GmbH, Taufkirchen, Germany	T1270
Vitamin B12	Sigma-Aldrich Chemie GmbH, Taufkirchen, Germany	V6629
(+/-)-α-Lipoic Acid (=Thiotic Acid)	Sigma-Aldrich Chemie GmbH, Taufkirchen, Germany	T1395
Vitamin C	Sigma-Aldrich Chemie GmbH,	A4034

	Taufkirchen, Germany	
Retinol/ Retinylacetate	Sigma-Aldrich Chemie GmbH, Taufkirchen, Germany	R7632
DL-Tocopherol/-acetate	Sigma-Aldrich Chemie GmbH, Taufkirchen, Germany	T1539_25mg
Linolic Acid/Liolenic Acid	Sigma-Aldrich Chemie GmbH, Taufkirchen, Germany	L1012
L-Cysteine HCI	Sigma-Aldrich Chemie GmbH, Taufkirchen, Germany	C7477
Glutathione	Sigma-Aldrich Chemie GmbH, Taufkirchen, Germany	G6013
Na-pyruvate	Sigma-Aldrich Chemie GmbH, Taufkirchen, Germany	P3662
Glutamine/Vitamin C	Sigma-Aldrich Chemie GmbH, Taufkirchen, Germany	G8540
Tris	Sigma-Aldrich Chemie GmbH, Taufkirchen, Germany	154563
Acetic acid	EM SURE® Merck kGaA, Darmstadt, Germany	K43073263 202
TUNEL® assay (In Situ Cell Death Detection Kit)	Roche, Mannheim, Germany	1215679291 0
ABC Kit	Vector Lab, Burlingame, CA, USA	H-3300
Biotin-Block-Kit	Vector Lab, Burlingame, CA, USA	SP-2001
Trizma base	Sigma-Aldrich Chemie GmbH, Taufkirchen, Germany	T-1503
Triton X-100	Sigma-Aldrich Chemie GmbH, Taufkirchen, Germany	X-100
Magnesium chloride	Sigma-Aldrich Chemie GmbH, Taufkirchen, Germany	M-2670
Biotinylated NAD	Trevigen	4670-5000-

		01
HEPES	Sigma-Aldrich Chemie GmbH, Taufkirchen, Germany	H-3375
KCl	Merck	1.04933
$MgCl_2$	Sigma-Aldrich Chemie GmbH, Taufkirchen, Germany	M-2670
$CaCl_2$	Sigma-Aldrich Chemie GmbH, Taufkirchen, Germany	C-3306
CMAC, t-BOC-Leu-Met	Molecular Probes	A-6520

Table 3.Antibodies used in immunohistochemistry

Primary Antibodies: mAb, pAb, Gt: goat, Ms: mouse, Rb: Rabbit.

Antigen	Host	Source/Cat.number	IHC
Actin	Ms, mAb	Milipore Billerica, MA, USA/mab1501	1:200
Actin	Rb, pAb	Abcam, UK/ab 1801	-
Avidin-Alexa 488	-	Molecular Probes, USA/ A-21370	1:80
Cleaved Caspase-3	Rb, mAb	Cell Signaling, USA/9665	1:400
PARP	Ms, mAb	BD Bioscience, San Jose, CA/ 556362	-
PAR (10H)	Ms,mAb,IgG3	Gene Tex, CA,USA/ GTX75054	1:200

Media and Buffers

0.1 M PB (Phosphate buffer)

- Solution A. 6.89 g NaH_2PO_4 x H_2O in 250 ml distilled ddH_2O (0.2 M)

- Solution B. 14.19 g NaH_2PO_4 in 500 ml ddH_2O (0,2M)
- Add A in B to reach a pH of 7.4
- 0.1 M PBS (Phosphate buffered saline)
- Dilute PB stock solution in ddH_2O (1:20), to have 0.01 M PB
- Add 9 g / liter of NaCl to have 0.01 M PBS

50 mM TBS (tris buffered saline)

- 6 g Tris in 900 ml ddH_2O
- Adapt pH to 7.6
- Complete until 1000 ml with ddH_2O
- Add 9 g / liter of NaCl

4 % Paraformaldehyde (PFA)

- 12 g PFA +150 ml PB
- Place it in the 60℃ for 45 min
- Add PB to dissolve until clear
- Room temperature: Add 280ml PH 7.4 into NaOH
- Dissolved to 300ml

10% Sucrose

- 20 g Sucrose dissolved in 200 ml PB

20% Sucrose

- 40 g Sucrose dissolved in 200 ml PB

30% Sucrose

- 60 g Sucrose dissolved in 200 ml PB

Basal medium (R16)

First, R16 powder was dissolved in 500 ddH_2O and 32.5 mM $NaHCO_3$, 30 / 60 nM $NaSeO_3$ X $5H_2O$, 5 nM $MnCl_2$ X $4H_2O$, 10 / 20 nM $CuSO_4$ X $5H_2O$ and 1 ml of 1 µg / ml Ethanolamine and 0.1 µg / ml Biotin were added in the same solution and filled up to a volume of 800 ml. Then the mixture was filtered and aliquoted into a volume of 50 ml.

Complete medium (Amount for 50 ml)

0.2% BSA, 50 µl Transferrin, 50 µl Progesterone, 50 µl Insulin, 50 µl T3, 50 µl Corticosterone, 50 µl Thiamine HC1, 50 µl Vitamin B12, 100 µl (+/-)-a-Lipoic Acid (=Thiotic Acid), 50 µl Retinol / Retinylacetate, 100 µl DL-Tocopherol / -acetate, 100 µl Linolic Acid/Linoleic Acid, 50 µl L-Cysteine HC1, 50 µl Glutathione, 50 µl Na-pyruvate, 0.5 ml Glutamine / Vitamin C, 6.15 ml ddH_2O were added into 40 ml Basal R16 Medium.

Proteinase K

To dissolve 250 mg Proteinase K Powder into 2.5 ml ddH_2O. Afterwards, dissolve 2.4 ml Proteinase K in 200 ml Basal medium and prepare 2 ml aliquot to for later use.

2.2 Methods

2.2.1 Animal procedures

All *Pde6a* mutants used were of the C57BI6 / J strain. The *Pde6a*^{V685M} and *Pde6a*^{D670G} mice were obtained from the Jackson Labs (Bar Harbor, MA, USA). The *Pde6a*^{R562W} mice were generated by *GenOway* (Lyon, France). *Pde6a*^{V685*R562W} compound heterozygous mice were generated at the University of Tübingen. All procedures were approved by the Tübingen University committee on animal protection and performed in compliance with the ARVO statement for the use of animals in Ophthalmic and Visual Research. Protocols compliant with the German law on animal protection were reviewed and approved by the ‘‘Einrichtung fur Tierschutz, Tierarztlichen Dienst und Labortierkunde’’. All efforts were made to minimize the number of animals used and their suffering.

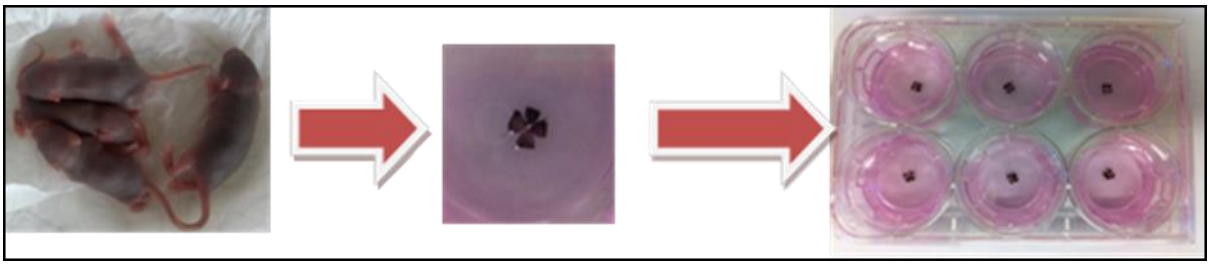

Figure 8.Retinal explants cultures

Retinas from Pde6a mutants were cultured at P25, P19, and P15 respectively. Before being treated with PJ34, the explants were allowed to adjust to in-vitro culturing conditions for 2 days. The cultures got treatments from P9 to P25-P19 and P15 respectively. Complete Medium without PARP inhibitor was used as the control.

Retinal explant culture procedure

All *Pde6a* animals for culturing were decapitated at postnatal day 5. After cleaning the heads with 70% ethanol, the eyes were removed under aseptic conditions, and placed into the Basal Medium for washing for 5 minutes followed by a 8-10 minute incubation in 0.12% Proteinase Kat 37℃ in order to inactivate the enzyme action by protein

dilution. After this step the eyes were placed in Basal Medium with 10% FCS (Fetal Calf Serum) for 2 minutes to deactivate the Proteinase K. The eyes were placed in Basal Medium during the whole procedure. The anterior segment, lens and vitreous body were removed from the eyeballs carefully. The optic nerve was then cut. Afterwards, the retinas were removed from sclera together with the attached retinal pigment epithelium. Then the retinas were cut into four wedge shapes. Afterwards the retinas were transferred to a 0.45 μm Cell culture Plate inserts (Mill cell, Cell Culture Inserts, 30mm Diameter, Merck Millipore Ltd. Tüllagreen, Germany), and were butterflied open with the ganglion cell layer facing up. Subsequently, the membrane was placed in a six well culture plate (Falcon, BD Biosciences, and San Jose, CA, USA) and incubated in 1.3 ml of Complete Medium at 37 ℃ in an incubator with humidity and 5% CO_2. All steps were done under the microscope and under sterile conditions.

2.2.2 Tissue Preparation (Embedding and section)

Prepare before

- 70% Ethanol
- 4% Paraformaldehyde (PFA)
- PBS (0.1 M; PH7.4)
- Sucrose (10%, 20%, 30%)
- Liquid nitrogen (Liquid N_2)
- Compound embedding (Tissue-Tek)

Procedure

Pde6a mice (P9-P35) mice were sedated with CO_2 and then decapitated. The heads were cleaned with 70% Ethanol, and the eye was removed. Subsequently, the eyes were punctured at the nasal part of the eye and incubated in 4 % PFA for 45 minutes at room temperature (RT). After washing in PBS (0.1M; PH 7.4), the cornea was cut along the limbus, then the Cornea, Lens, and vitreous were removed, and put in 4% PFA for 45 minutes at RT. After washing in PBS 3 times for 10 minutes, the eyecups were kept for 10 minutes in 10% sucrose, 20 minutes in 20% sucrose and 30 minutes in 30% sucrose

at room temperature. After cryo-protection, the tissues were embedded in O.C.T™ compound (Tissue-Tek, Leica, Bensheim, Germany), and immediately frozen in liquid nitrogen and then stored at -20℃ until sectioning. For unfixed tissues, the eyes were quickly and directly frozen in liquid nitrogen followed by embedding in O.C.T™ cryomatrix, and then stored in the -20℃.

2.2.3 Dissection of retina

Prepare before

- 70% Ethos
- 4% Paraformaldehyde (PFA)
- PBS (0.1 M; PH 7.4)
- Sucrose (10%, 20%, 30%)
- Liquid nitrogen (Liquid N_2)
- Compound (Tissue-Tek)

Procedure

The eyes were enucleated and fixed in 4% PFA for 45 minutes. Subsequently, the retinae were washed in PBS (0.1 M, PH 7.4) for 5 minutes. Then cryo-protection was performed by submergence in 10% sucrose for 10 minutes, 20% sucrose for 20 minutes, and 30% for 30 minutes. Afterwards, the retinae were embedded in O.C.T™ compound (Tissue-Tek, Leica, Bensheim, Germany) and were stored at -20℃. The retinae blocks were sectioned sagittally with 14 μm thicknesses by using a microtome (Leica RM 2155, Nussloch, Germany) and then the slides were stored at -20℃ for further experiments.

2.2.4 TUNEL (In Situ Cell Death Detection Kit) assay

The TUNEL assay is a common method for detecting DNA fragmentation which is one of the last steps of cell death. Because of the presence of a fluorescein, nucleotide polymers can be detected and quantified by fluorescence microscopy (Gavrieli, Sherman et al. 1992).

Prepare before

- Proteinase-K Dilution

Proteinase-K	1×	2×	3×
0.05M Tris PH 7.6	42 ml	84 ml	100 ml
Proteinase-K	6 µl	12 µl	14.3 µl

- Ethanol-Acetic Acid-Mix

70% Ethanol	49 parts
30% C2H4O2	9 parts
H_2O	21 parts

- Blocking solution

10% NGS
1% BSA
1% fish gelatin
0.003% PBST

- TUNEL-Kit

Solution	Components	For 100 µl
Enzyme (blue)	Terminal deoxynucleotidyl transferase (TdT) from calf thymus, recombinant in E. coli	6.25 µl
Label (Lila)	Nucleotide mixture in reaction buffer	56.25 µl
Blocking solution	See above	62.50 µl

Procedure

Fixed slides were dried at 37℃ for 40 minutes, and were washed in PBS at room temperature for 15 minutes. Afterwards, the slides were placed in Tris + Proteinase K at 37℃ for 5 minutes to inactive nucleases, which may reduce the nucleic acids. Then the slides were washed with Tris (10 µg / ml in 10 mM TRIS-HCL, pH 7. 4 – 8. 0) 3 for 5 minutes. Subsequently, the slices were placed in Ethos-Acetic Acid-Mix at -20℃ for 5

minutes and then blocked with blocking solution for 1 h at room temperature. Lastly, the slides were placed in the TUNEL kit (Fluorescein or TMR; Roche Diagnostics GmbH, Mannheim, Germany) in 37 ℃ for 1h and covered with Vectashield with DAPI (Vector, Burlingame, CA, USA) thereafter.

2.2.5 Caspase 3 immunostaining

For immunofluorescence analysis, retinae sections were rinsed in PBS and incubated in blocking solution (10% normal goat serum, 1% bovine serum albumin, and 0.1% Triton X in PBS) for 1hour at room temperature. Sections were incubated with an antibody directed against cleaved activated Caspase-3 (1:400, Cell Signalling Technology, USA; Orders. 877-616-CELL 2355), which was diluted in blocking solution overnight at 4℃. Subsequently, sections were washed in PBS and mounted in Vectashield with DAPI (Vector, Burlingame, CA, USA).

2.2.6 Calpain activity Assay

Calpain is a type of Ca^{2+} activated protease which activate when the levels of Ca^{2+} increase (Azarian, Schlamp et al. 1993). The permeable fluorescent Calpain substrate, tert-butoxycarbonyl-L-leucyl-Lmethionineamide-7-amino-4-chloromethylcoumarin (Boc-Leu-Met-CMAC), was used to assess Calpain activity at the cellular level in photoreceptors of *Pde6a* mutants.

Prepare before

- Calpain Reaction mix

Volume	Stock		Working concentration
1000 µl	Ready to use (HEPES 25 mM 5.96 g; KCL 65 mM 4.85 g,$CaCl_2$ 15 mM 0.22 g, 2 mM $MgCl_2$, 60 ml ddH_2O) 10 ×	Reaction buffer (CRB 1×)	Adjust PH to 7.2 and complete the volume to 100 ml with ddH_2O
2 µl	1 mM	DTT	1 µl
5 µl	10 µM	CMAC	5 µl

Procedure

Unfixed retinal slides were dried at room temperature for 10 minutes and then washed with CRB for 15 minutes. Thereafter, the 1×CRB+CRM (Calpain reaction mix) was added to the slides and incubated for 2 h in the 37℃ incubator. Lastly, the slides were washed with 1 × CRB for 2 × 10 minutes and kept in the dark. Finally, the slides were covered with Vectashield without DAPI (Vector, Burlingame, CA, USA).

2.2.7 Poly ADP ribose polymerase In-situ Enzyme activity Assay (PARP)

Prepare before

- TB 100 mM, PH8.0
- 12.14 g Trizma base dissolve in 600 ml ddH_2O
- PH 8.0 With 2NHCL
- Fill to 1000 ml with ddH_2O
- PARP reaction buffer (PRB)
- TB, 0.2%Triton, 10 mM $MgCL_2$
- 250 ml Trisma Base
- 500 µl Triton * 100
- 0.508 g $MgCL_2$ dissolve
- Heat the oven to 37℃
- Set the PARP reaction mix Dithiothreitol (DTT) Stock solution, 1 M
- 154.25 mg dissolve in 1 ml ddH_2O

PARP reaction mix

Name	Stock solution	Working concentration	Volume
Reaction buffer (RB)	100 mM TB PH 8.0 0.2%Triton, 10 mM $MgCl_2$	-	980 µl
DTT	1 M	1 mM	1 µl
Biotinylated NAD	250 µM	5 µM	20 µl

Procedure

The unfixed retinae tissue were air-dried at room temperature for 10 minutes and subsequently washed in TB (Tris base buffer 100 mM PH 8.0; 4℃) for 10 minutes. Afterwards, the slides were placed in cover-plates and washed with a 1 × TB buffer. Subsequently, Avidin Block was placed on each slide (3 drops / slide) and left for 15 minutes. Thereafter, washing with TB 2 × 5 minutes followed this step. Again, a few drops were added of Biotin Block to each slide (3 drops / slide) for 15 minutes. The slides were washed with TB 2 placed on each slide (3 drops / slide) and left for 15 minutes. Afterwards, a PARP reaction mix was applied in 37℃ for 2.5 h, and later washed with PBS 3 x 5 min. For detection of incorporated biotin, Alexa 488, Avidin 1:800 in PBS was applied for 1 hour and followed by washing in PBS. Lastly, the slides were covered with Vectashield with DAPI (Vector, Burlingame, CA, USA).

2.2.8 Poly (ADP-ribose) (PAR) immunohistochemistry

Prepare before

- PAR Quenching

Name	Working concentration	Volume
PBST	1: 1000	500 µl
MeOH	400 µl 70%	400 µl
H_2O_2 (Hydrogen peroxide)	30 : 100	100 µl

- Blocking solution

Stock solution	Working concentration	Volume
PBST	1: 1000	1000 µl
NGS	1: 10	100 µl

- Prepare PAR-Primary antibody

Name	Source	Dilution	Working concentration
PAR (10H)	Enzo / ALX-804-220, Ms, mAb	1 : 200	4 µl

- Prepare PAR-secondary antibody

Name	Source	Dilution	Working concentration
Biotinylated lgG (H+L)	Vector Laboratories, CA, USA, Gt anti Ms	1 : 150	6 µl

- Prepare ABC kit

Name	Information	Source	Dilution	Working concentration
Avidine	Gt anti Ms	Vector Laboratories, CA, USA	1 : 150	1 µl
Biotin		Vector Laboratories, CA, USA		1 µl

Procedure

For this immunohistochemistry assay, the fixed cryo-sections were dried at 37 ºC for 1 h, and then washed with PBS for 10 min at room temperature. To reduce non-specific background, quenching solution (100 µl 30% H_2O_2, 400 µl Methanol 500 µl PBST) was placed in each section for 20 min at room temperature. Then, blocking solution (10% NGS, 0.1% PBST) blocked the slices for 1 h at room temperature. Thereafter, the slides were incubated with primary antibody (PAR 10 H, lgG3 Alex3 1 : 200) at 4℃ overnight. After that, the slides were washed with PBS 3 times for 10 min, and then were incubated with the second antibody (Biotinylated goat anti mouse, 1 : 150) at room temperature for 1 h. After the washing step, slides were incubated in Vectastain Elite ABC kit (Vector lab) for 1 h at room temperature. The slides were placed in a solution which included 40 mg 3, 3'-diaminobenzidine (DAB), 20% Glucose, 0.4% Nickel ammonium sulphate, 40 µl Glucose oxidase and incubated for 3 min for the colour reaction. After they were washed by PB 3 times for 10 min. Slides were covered with by Aquatex (Merck).

2.2.9 Microscopy, cell counting, and statistical analysis

Light and fluorescence microscopy were performed with a Z1 Apo Tome Microscope equipped with a Zeiss Axiocam digital camera. Images were captured using Zeiss Axiovision 4.7 software and representative pictures were taken from central areas of the

retina. Adobe Photoshop CS3 (Adobe Systems Incorporated, San Jose, CA) and Corel Draw X3 software was used for primary image processing. For cell quantifications, pictures were captured of whole radial slices using the Mosaix mode of Axiovision 4.7. Labelled cells were counted manually. The total number of cells was determined by dividing the outer nuclear layer (ONL) area through the average cell size. The total number of ONL cells was determined by taking the percentage of positive cells then dividing the number of positive cells. All data given represent the means and standard deviation from three sections each, for at least three different animals. Statistical comparisons between experimental groups were made using one-way ANOVA and Bonferroni's correction using Prism 5 for Windows (Graph Pad Software, La Jolla, CA). Values are given as mean ± standard deviation (SD) or standard error of means (SEM). Levels of significance were as follows: n.s., $p > 0.05$; *, $p < 0.05$; **, $p < 0.01$; ***, $p < 0.001$.

3. Results

3.1 Characterization of four *Pde6a* mutants *in vivo*

3.1.1 The peak of photoreceptor cell death in different Pde6a mutants in vivo

Programed cell death relates to the orderly process of changes in cell morphology and biochemistry that finally results in cell death (Kerr, Wyllie et al. 1972). A variety of programmed cell death mechanisms are known, including apoptosis, programmed necrosis, necroptosis, and PARthanatos (Leist and Jaattela 2001). TUNEL (Terminal deoxynucleotidyl transferees dUTP nick end labeling) is a common method to detect DNA fragmentation as end result of apoptosis but also of other forms of cell death, for instance in necrosis (Loo 2002). We used the TUNEL cell death assay to identify photoreceptor cell death in different models for *Pde6a* mutation, and we found that cell death starts at P9 in $Pde6a^{V685M}$, $Pde6a^{V685M*R562W}$, *and* $Pde6a^{R562W}$ and at P14 in $Pde6a^{D670G}$. Thus, TUNEL staining showed retinal photoreceptor cell death in early stages and it was significantly elevated from P9 onwards in 4 different *Pde6a* animal models.

Overall, TUNEL positive cells were identified as late as PN30 in four *Pde6a* mutants. In wild type *wt* (C3H) controls, TUNEL positive cells were seen only occasionally in the ONL at this age (Figure 9). Compared to *wt* retinae, $Pde6a^{V685M}$ retinae showed a significant elevation of photoreceptor cell death at PN12 (Table 3). The photoreceptor degeneration in the $Pde6a^{V685M}$ mutant was the earliest compared to other *Pde6a* mutants. The TUNEL positive cells peaked at PN12 in $Pde6a^{V685M}$ while in $Pde6a^{D670G}$ the TUNEL peak was at PN21. In other *Pde6a* mutants, TUNEL-positive cells peaked at PN15 for $Pde6a^{R562W}$ and $Pde6a^{V685M*R562W}$ and all *Pde6a* mutants showed significantly higher numbers of TUNEL positive cells than wild type animals (Figure 9).

In these *Pde6a* models, photoreceptor rows showed the highest number at PN9 (11 ONL cell rows remaining), declining thereafter. Dying cells and photoreceptor cell rows were quantified until PN35 (Table 3, Figure 9).

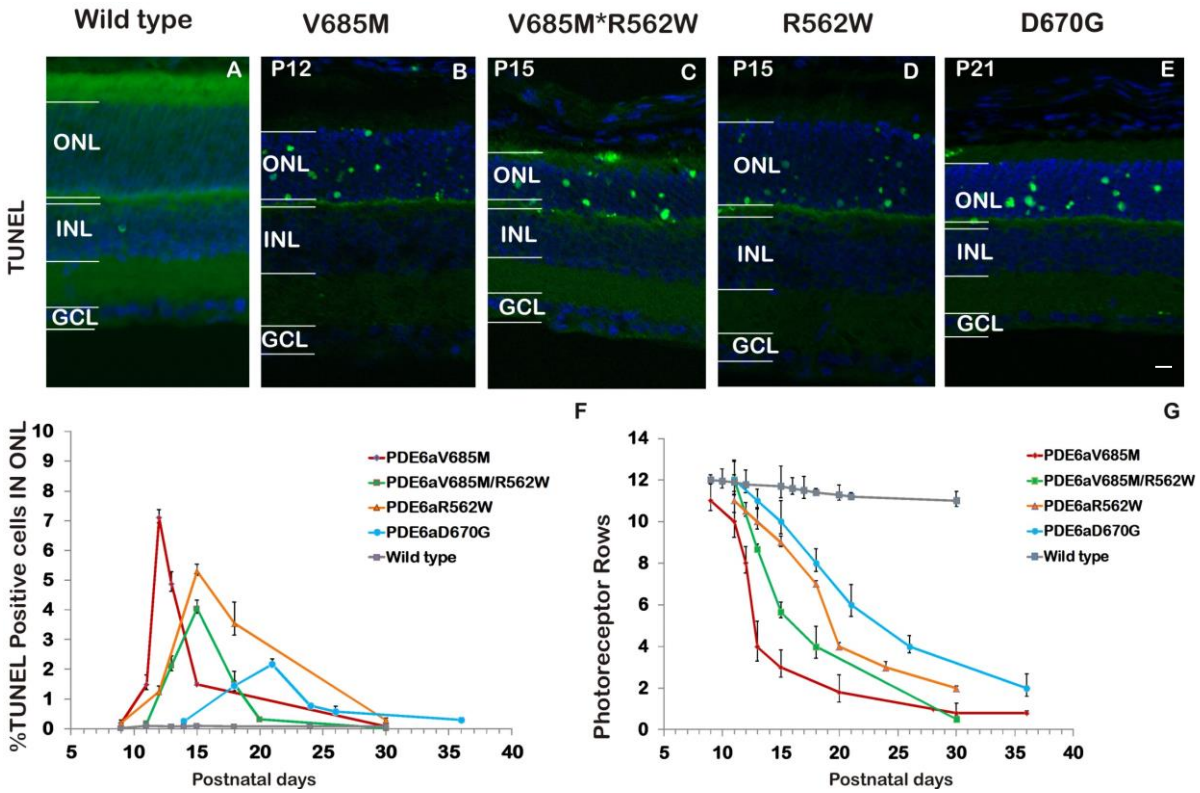

Figure 9. TUNEL assay and cell death in Pde6a mutants

The number of TUNEL positive cells in the 4 different *Pde6a* mutants ONL was strongly increased when compared with wt (A-E). Quantification of photoreceptor cell death and photoreceptor rows during the first 35 postnatal days (F, G). Increased numbers of TUNEL positive cells, showing a peak at PN12 in $Pde6a^{V685M}$, PN15 in $Pde6a^{R562W}$, PN15 in $Pde6a^{V685M*R562W}$ and PN21 in $Pde6a^{D670G}$ was observed (F). Quantification of photoreceptor rows during the first postnatal month. In $Pde6a^{V685M}$, photoreceptor rows showed the highest number at PN9 (11 ONL cell rows remaining), declining thereafter. In the other three mutants the photoreceptor rows showed the highest number at PN11 (11 ONL cell rows remaining), declining thereafter. In the *Pde6a* models, dying cells and photoreceptor cells rows were detectable as late at PN35 (G). The values shown originate from four *Pde6a* mutants from at least three different specimens. Scale bar represents 20 µm.

3.1.2 Cell death in Pde6a mutants

Caspase-3 is a critical executioner of apoptosis, as it is either partially or totally responsible for the proteolytic cleavage of many key proteins, such as the nuclear enzyme poly (ADP-ribose) polymerase (PARP)(Casao, Mata-Campuzano et al. 2015). Since photoreceptor cell death in retinal regenerations is frequently defined as apoptosis; the detection of activated Caspase-3 by an antibody that is specific to the activated form of Caspase-3 was used to analyze real involvement of apoptotic photoreceptor cell death in *Pde6a* mutants. However, only a few cells with activated Caspase-3 were seen in ONL of each *Pde6a* model, and there were no significant difference between the controls and the *Pde6a* mutants (Table 3, Figue10), indicating that the staining only correspond to developmental cell death. Thus, we discarded apoptosis as the main cell death pathway in these mutants.

3.1.3 Calpain activity is increased in Pde6a mutants and wild type retina in vivo

The activation of Ca^{2+}-dependent protease Calpain has been implicated in retinal neurodegeneration, and it is usually associated with alternative cell death mechanisms (Paquet-Durand, Azadi et al. 2006, Paquet-Durand, Sanges et al. 2010). Photoreceptor degeneration in most mutations of RP often affects rods first and then cones through an unknown cell death pathway (Delyfer, Leveillard et al. 2004). The localization of Calpain activity is of major importance both for our understanding of the degenerative mechanisms and the assessment of potential neuroprotective treatments (Paquet-Durand, Johnson et al. 2007).

So far, still no publications have addressed the role of Calpain activity in retinal degeneration of a *Pde6a* mutant. Here we reported four different *Pde6a* animal models.

In the *Pde6a* mutants, numerous photoreceptors in the ONL were nicely labeled with our assay for Calpain activity, but in wild-type animals very few positive cells were observed. The numbers of cells showing Calpain activity in $Pde6a^{V685M}$ ONL were higher at various postnatal ages as compared to the wild type. Calpain activity was increased early at P9 and peaked at P12 (Table 3). The $Pde6a^{V685M*R562W}$ retinae showed comparatively higher number of cells with activated Calpain when compared to the wild type; the peak of the Calpain positive cells was at P15 (Table 3). Calpain activity in

Pde6a^{R562W} appeared as early as at P11, the number of Calpain positive cells peaked at P15 (Table 3). In the *Pde6a*^{D670G} mutant, the increase of Calpain activity was found at P14 and showed statistical significance at P18, and peaked at P21 (Table 3) with a later decrease at P24 (Figure10).

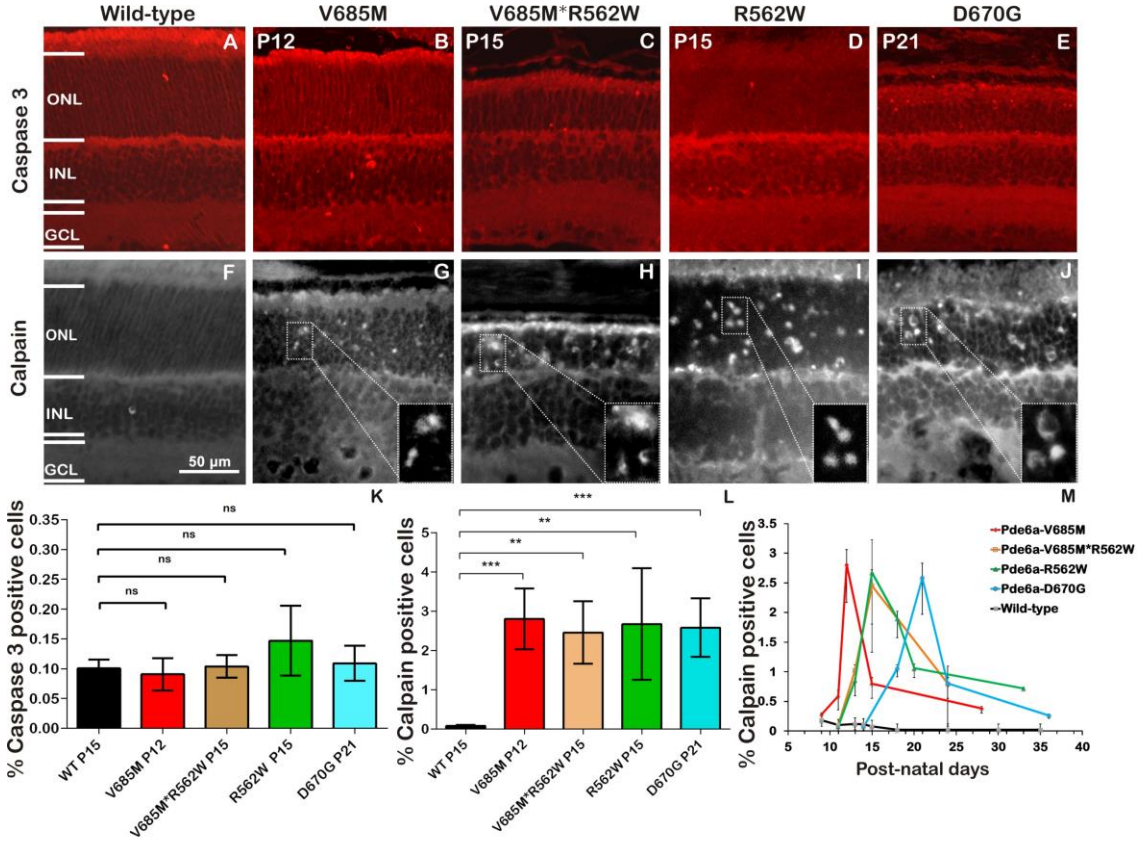

Figure 10.Activation of Calpain and Caspase-3 assay in Pde6a mutants

Photoreceptor degeneration in *Pde6a* mutants correlates with Calpain activity, however activation of Caspase-3 was not detected in these animals. Immunofluorescence for activated Caspase-3 reveals no major differences between wild-type and mutant retinae (A-E). This is also illustrated by the quantification of Caspase-3 positive cells, which shows low numbers of positive cells at the respective peaks of degeneration (K). In contrast, the in situ Calpain activity assay reveals strong differences between wild-type (F) and all four *Pde6a* mutant situations (G-J). The progression of Calpain activity was analyzed over time (L, M) and shows a strong correlation to the retinal degeneration. The values shown originate from four *Pde6a* mutants from at least three different specimens. Scale bar represents 50 µm.

3.1.4 PARP activity in Pde6a mutants in vivo

In order to investigate the involvement of PARP as a latent photoreceptor cell death marker in these *Pde6a* mutants, we studied the expression and activation of PARP. This may allow us to identify opportunities for treatment of RP patients in the future. PARP activity at the cellular level was detected utilizing an in-situ enzyme activity assay that detects the incorporation of biotin labeled NAD^+ (Paquet-Durand, Silva et al. 2007).

In wild-type retinae, very little PARP activity was detected. In comparison to *wt*, PARP activity in $Pde6a^{V685M}$ peaked at P12. And in $Pde6a^{V685M*R562W}$, $Pde6a^{R562W}$ and $Pde6a^{D670G}$ PARP activity showed a peak at P13, P15 and P21 respectively and the number of PARP positive cells was significantly different than *wt* (Table 3,Figure 11,12).

3.1.5 PARylated proteins in Pde6a mutants in vivo

We quantified the amount of PARylated protein in the four *Pde6a* mutants. The quantification of PARylated protein showed increased poly(ADP)-ribosylation of proteins in each *Pde6a* mutant's photoreceptors. In comparison to *wt*, the statistical analysis of PAR positive cells showed significant differences for $Pde6a^{V685M}$ at P12, $Pde6a^{V685M*R562W}$ at P15, $Pde6a^{R562W}$ at P15, $Pde6a^{D670G}$ at P21 (Table 3) (Figure 11P-T, 12F).

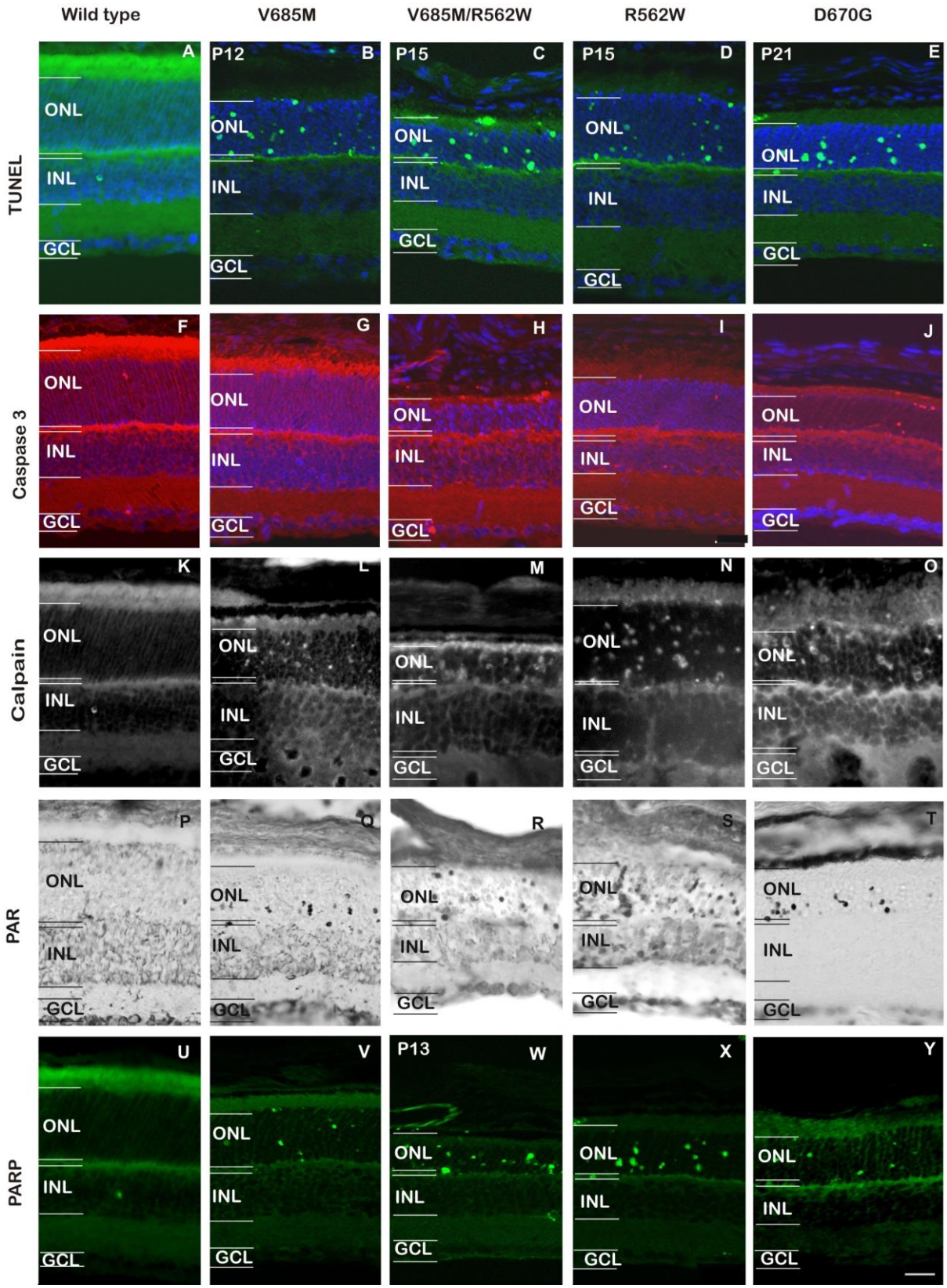
Wild type
V685M
V685M/R562W
R562W
D670G
TUNEL
Caspase 3
Calpain
PAR
PARP
A
B
C
D
E
F
G
H
I
J
K
L
M
N
O
P
Q
R
S
T
U
V
W
X
Y
P12
P15
P15
P21
P13
ONL
INL
GCL

Figure 11. Differential regulation of markers linked to cell death in *Pde6a* mutants

The presence of DNA nick-ends and the presence and activity of the three enzymes Caspase-3, Calpain, and PARP, linked to cell death were analyzed. Shown here are: TUNEL assay for cell death (A-E) Presence of activated Caspase-3 for apoptotic cell death (F-J), *in situ* Calpain activity assay for non-apoptotic cell death (K-O), PARylated protein immunohistochemistry for non-apoptotic cell death (P-T), and *in situ* PARP activity assay for non-apoptotic cell death (U-Y). Although there was no significant difference between *wt* and *Pde6a* mutants for the presence of Caspase-3, there were significant differences between *wt* and *Pde6a* mutants for nick-ends in the DNA (*i.e.* cell death), Calpain activity, the presence of PARylated protein and the activity of PARP. Scale bar = 20 μm.

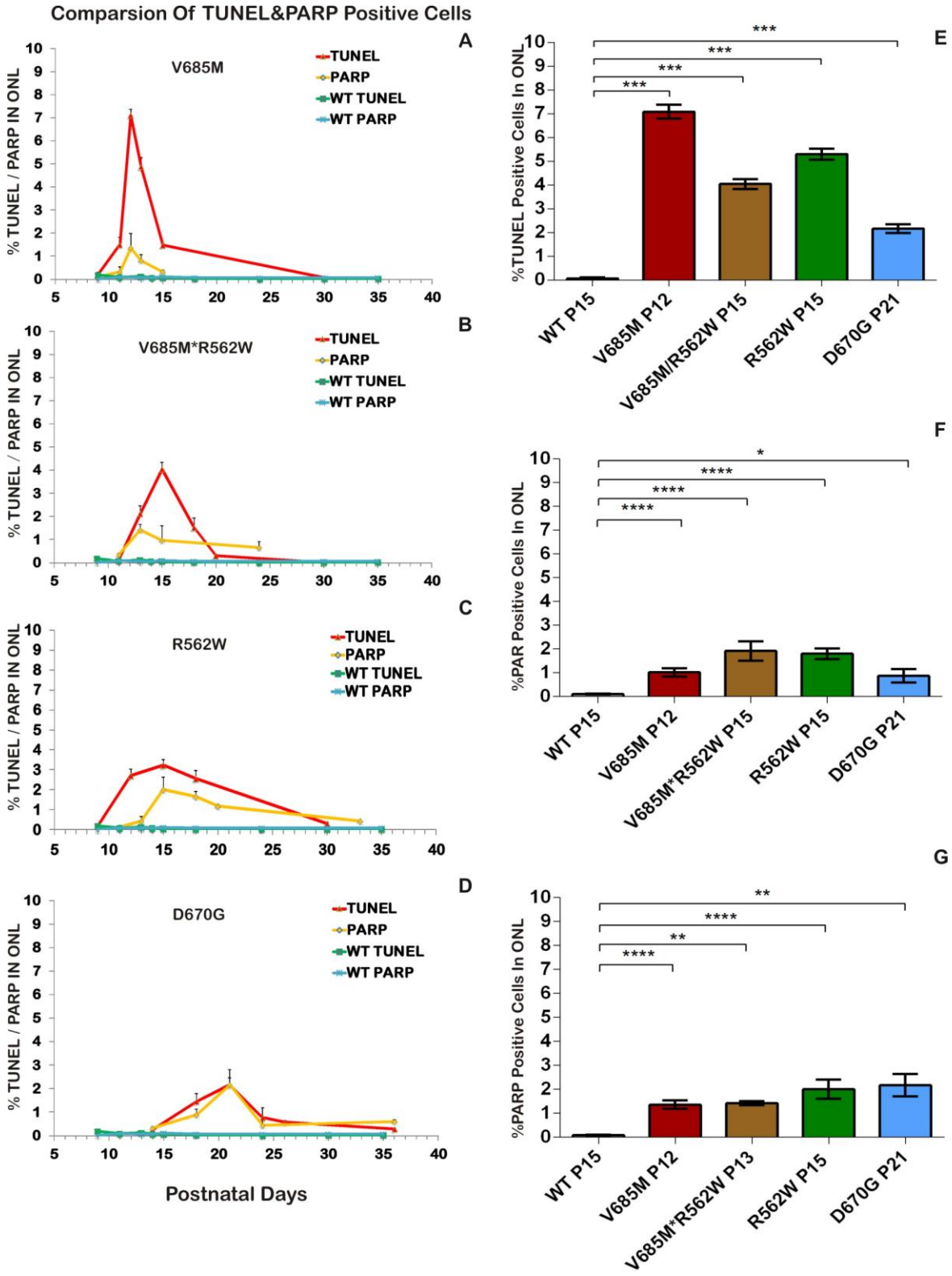
Comparsion Of TUNEL&PARP Positive Cells
A
V685M
TUNEL
PARP
WT TUNEL
WT PARP
% TUNEL / PARP IN ONL
B
V685M*R562W
C
R562W
D
D670G
Postnatal Days
E
%TUNEL Positive Cells In ONL
WT P15
V685M P12
V685M/R562W P15
R562W P15
D670G P21
F
%PAR Positive Cells In ONL
V685M*R562W P15
G
%PARP Positive Cells In ONL
V685M*R562W P13

Figure 12. PARP activity and PARylation accumulation in different *Pde6a* mutants

The number of TUNEL-positive cells in the *Pde6a*^{V685M}, *Pde6a*^{V685M*R562W}, *Pde6a*^{R562W} and *Pde6a*^{D670G} photoreceptors was significantly increased when compared with *wt* (A-E). Progression of photoreceptor cell death in *Pde6a*^{V685M}, *Pde6a*^{R562W}, *Pde6a*^{V685M*R562W} and *Pde6a*^{D670G} showed a peak at P12, P15, P15 and P21 respectively. However, only a few Caspase-3 positive cells were seen in ONL of each *Pde6a* animal models, and there were no significant differences between *wt* and *Pde6a* mutants (F). PAR accumulation as secondary evidence of PARP activity was found in large amounts in ONL of each of the *Pde6a* mutants (G). The number of PARP activity-positive cells in *Pde6a* mutants was strongly increased when compared with *wt* (K-H). Progression of PARP activity at different time points showed a peak at P12, P13, P15, P21 for *Pde6a*^{V685M}, *Pde6a*^{V685M*R562W}, *Pde6a*^{R562W} and *Pde6a*^{D670G} respectively (A, B, C, D, H). The images shown are representative for observations on at least three different specimens for each genotype. *P<0.05.Scale bar = 20 μm.

3.1.6 Summary of characterization of Pde6a mutants in vivo

Our detailed characterization of different homozygous and compound heterozygous mouse models for RP provide not just a better view of the mechanisms of RP degeneration, but will also provide a base for investigations, in particular for the determination of the best possible time-frame for therapeutic interventions in the future.

Table 4.Characterization of *Pde6a* mutants *in vivo*

Animal	n	TUNEL	Caspase- 3	Calpain	PARP	PAR	Phot. rows
wt	6	0.07 ± 0.02	0.10 ± 0.01	0.08 ± 0.01	0.08 ± 0.02	0.11 ± 0.01	11.24 ± 0.48
V685M	6	7.09 ± 0.14 (***)	0.09 ± 0.01 (ns)	2.80 ± 0.45 (***)	1.36 ± 0.17 (***)	1.02 ± 0.07 (***)	3.90 ± 0.61 (***)
V685M* R562W	6	4.05 ± 0.10 (***)	0.10 ± 0.01 (ns)	2.46 ± 0.46 (**)	1.43 ± 0.08 § (***)	1.92 ± 0.23 (**)	5.67 ± 0.24 (***)
R562W	6	3.11 ± 0.74 (**)	0.15 ± 0.03 (ns)	2.66 ± 0.45 (**)	2.01 ± 0.40 (**)	1.80 ± 0.23 (***)	8.98 ± 0.16 (**)
D670G	6	2.17 ± 0.09 (***)	0.11 ± 0.01 (ns)	2.58 ± 0.43 (***)	2.17 ± 0.47 (**)	0.87 ± 0.28 (*)	6.09 ± 0.32 (***)

Summary of assay results in the four different *Pde6a* mutants in *vivo*, at the respective peak of cell death. (*V685M* at P12, *V685M*R562W* at P15, *R562W* at P15 and *D670G* at P21, always *vs*. *wt* P15 condition). TUNEL, Caspase-3, Calpain, PARP, PAR, Photoreceptor rows levels of significance were as follows: n.s.=p>0.05; *=p<0.05; **=p<0.01; ***=p<0.001. Parameters are presented as mean ± standard deviation (S.D). §=Postnatal 13.

3.2. Treatment of *Pde6a* mutants *in vitro*

3.2.1 PARP inhibition delays photoreceptor cell death in Pde6a mutants in vitro

Our *in vivo* study showed that the cells positive for assays of TUNEL and PARP activity in the ONL of *Pde6a* mutants were strongly increased when compared with *wt in vivo*. In addition, in our previous study, 6 µm PJ34 treatments showed neuroprotective effect for *rd1* photoreceptor degeneration (Paquet-Durand, Silva et al. 2007). In addition we used several concentrations of PJ34 for photoreceptor degeneration in the *rd2* slow degeneration model. We observed a neuroprotective effect of PJ34 for 1.5 µm and 6 µm PJ34 treatments (unpublished data). Furthermore, it was shown that adult PARP1 KO

mice retinae indicated normal structural and functional behavior (Sahaboglu, Tanimoto et al. 2010). This suggests that inhibition of PARP1 does not have a negative effect on retinal development and function. So, we hypothesized that PARP inhibition could decrease or delay photoreceptor cell death and increase photoreceptor survival in *Pde6a* mutants *in vitro*.

We used organotypic retinal cultures as an *in vitro* system to test our hypothesis. Retinae from *Pde6a* mutants were cultured and treated with PJ34. To assess the effective neuroprotection period of PJ34, we used long and short-term retinal culture periods using 6μM PJ34 as a treatment. First, long-term culture period (P5-P25) was used to analyze the neuroprotective effect of PARP inhibition on $Pde6a^{V685M}$, $Pde6a^{V685M*R562W}$ and $Pde6a^{D670G}$ retinae for 16 days. The results from treated groups showed hardly any photoreceptors in these *Pde6a* mutants in both treated and untreated groups, which lead us to believe they may have been degenerated already at such a stage. Therefore the quantification was impossible at P25 (*Data not shown*) (Figure 14). When culture protocol was shortened from P25 to P19, we observed a single layer of photoreceptors, and therefore, quantification was also not possible (*Data not shown*) (Figure 14). There was a significant difference between treated and untreated groups when cultures were finished at P15 (Figure 13). The number of photoreceptor rows in each *Pde6a* mutant was higher after treatment while there was only one layer of photoreceptor rows in the untreated group (Figure 14A-U).

We used the TUNEL assay to identify photoreceptor cell death for PJ34-treated and untreated *Pde6a* mutants. All *Pde6a* mutants demonstrated higher a number of TUNEL-positive cells in the untreated groups when compared to treated groups. PARP inhibition by PJ34 significantly decreased the number of photoreceptor cell deaths in $Pde6a^{V685M}$, $Pde6a^{R562W}$ and $Pde6a^{V685M*R562W}$ (Table 4, Figure 13).

3.2.2 PARP inhibition positively affected photoreceptor survival in Pde6a mutants in vitro

Short-term cultures were performed using P5 mice. The retinal cultures derived from Pde6a mutants were left for 4 days in regular R16 culture medium to adapt to the

culture situation. Every second day the culture medium was changed. Treatment with 6µM PJ34 was started at P9 for 6 days up to a total age of P15. PJ34 treatment revealed a significant increase in the number of surviving photoreceptors in treated *Pde6a*^{V685M*R562W} and *Pde6a*^{R562W} (Table 4), but there was no significant difference between treated and untreated *Pde6a*^{V685M} retinae (Table 4, Figure 13).

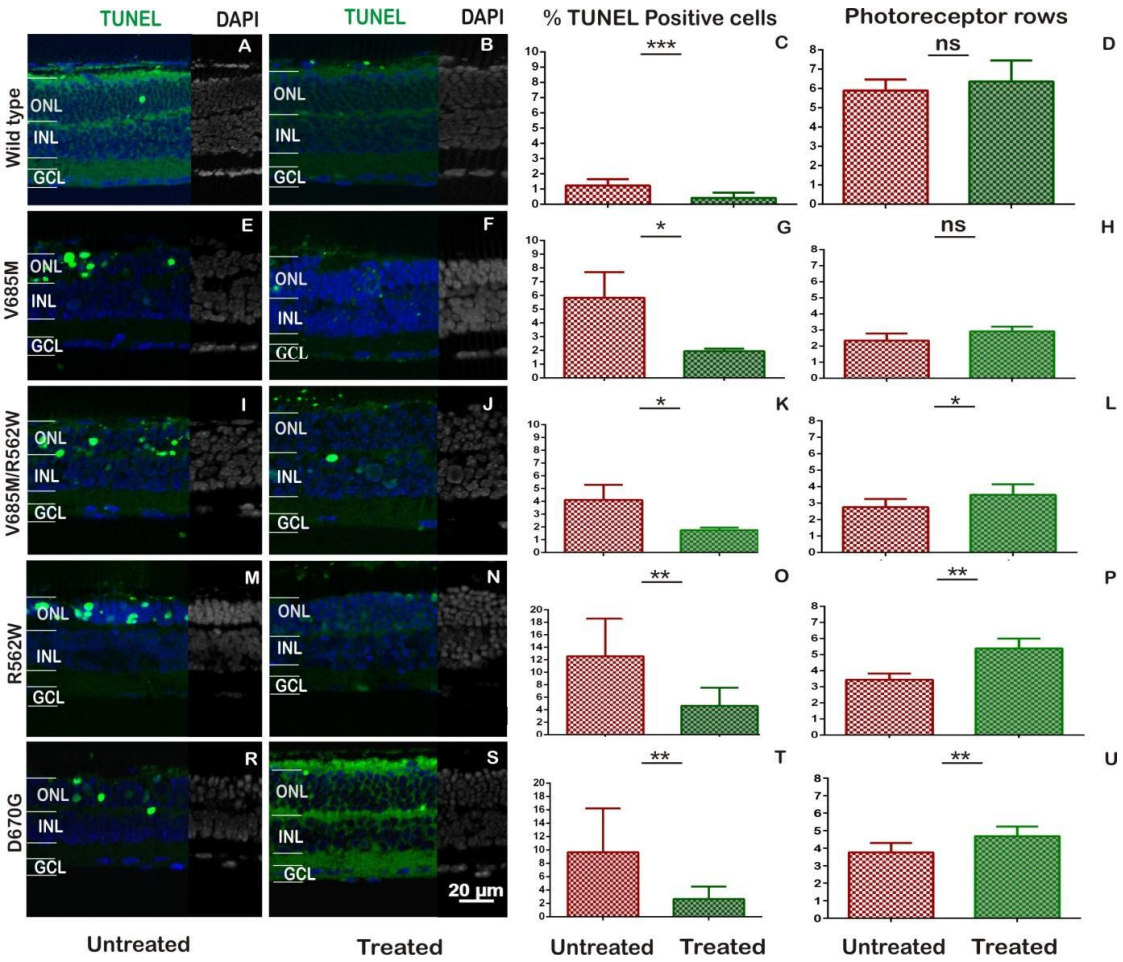

Figure 13. PARP inhibition in short-term cultures of *Pde6a* mutants

In short-term (P5-P15) cultures the number of TUNEL-positive cells in the *Pde6a*^{V685M}, *Pde6a*^{V685M*R562W}, *Pde6a*^{R562W}, *Pde6a*^{D670G} and *wt* ONL (A, E, L, M, R) was significantly decreased by PJ34 treatment (C, G, K, O, T), suggesting a protective effect of the PARP inhibitor. Treatment with PJ34 (P9-P15) resulted in a significant increase in the number of photoreceptor rows in *Pde6a*$^{V685M/R562W}$ *Pde6a*^{R562W} and *Pde6a*^{D670G} (J, N, L, P, U), but not in *Pde6a*^{V685M} and *wt* (B, F, D, H) when compared with untreated specimens; the staining were representative of six specimens; *P<0.05. Scale bar represents 20 um.

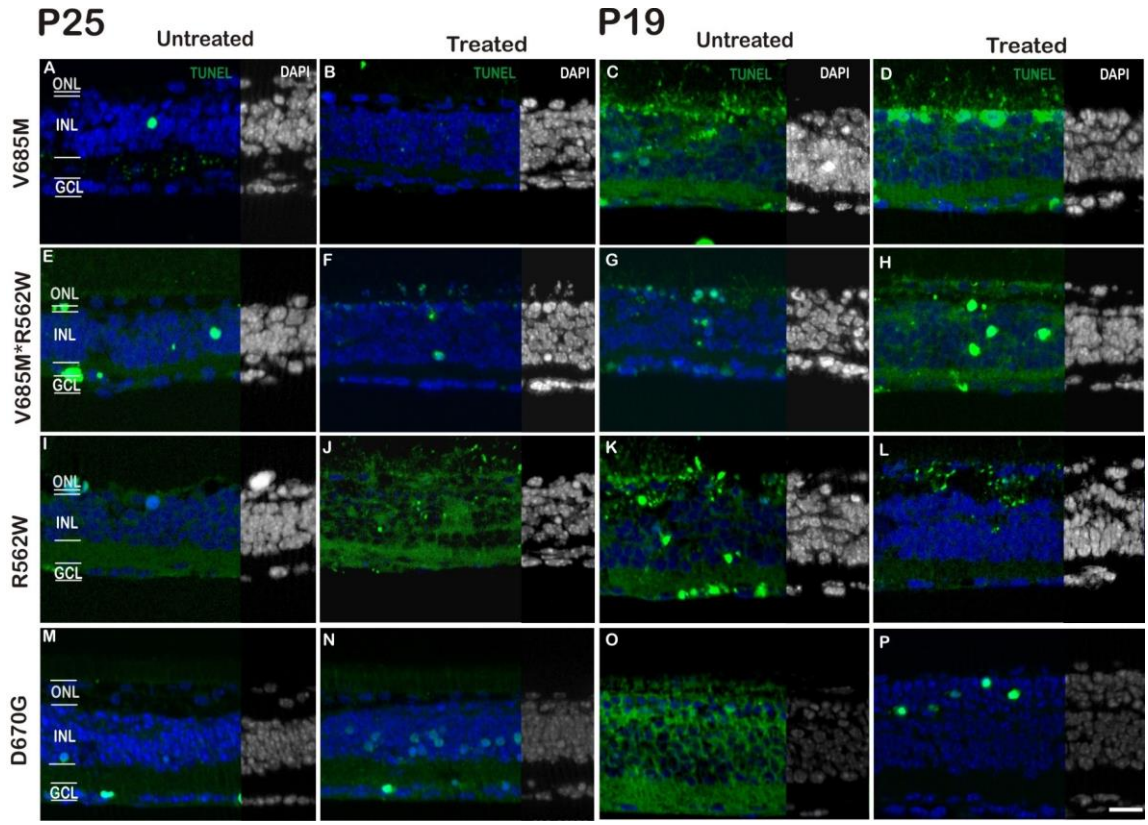

Figure 14. PARP inhibition in long-term cultures of *Pde6a* mutants

Long-term culture period (P5-P25) was used to analyze the neuroprotective effects of PARP inhibition on *Pde6a*^{R562W}, *Pde6a*^{V685M} *and Pde6a*^{V685M*R562W} retina for 16 days. The results from treated groups showed very few photoreceptors in all the *Pde6a* mutants in both treated and untreated groups and therefore the quantification was impossible at P25 (A, B, E, F, I, J, M, N). However, when culture protocol was optimized from P25 to P19, we observed only a single layer of photoreceptors, and therefore, quantification was not possible (C, D, G, H, K, L, O, P). The staining was representative of at least three specimens. Scale bar represents 20 µm.

3.2.3 PARP inhibition decreases Pde6a mutant PAR-positive cells in vitro

As PARP activity generates PAR polymers, staining for PAR polymers was performed in retinal tissues to indirectly confirm PARP activity. PAR polymer staining showed numerous cells with PAR polymers in the ONL of all *Pde6a* mutants. Our study showed

that the PARP inhibitor PJ34 could decrease the number of PAR polymers in the cells of the ONL of *Pde6a* mutants *in vitro* (Table 4, Figure 15).

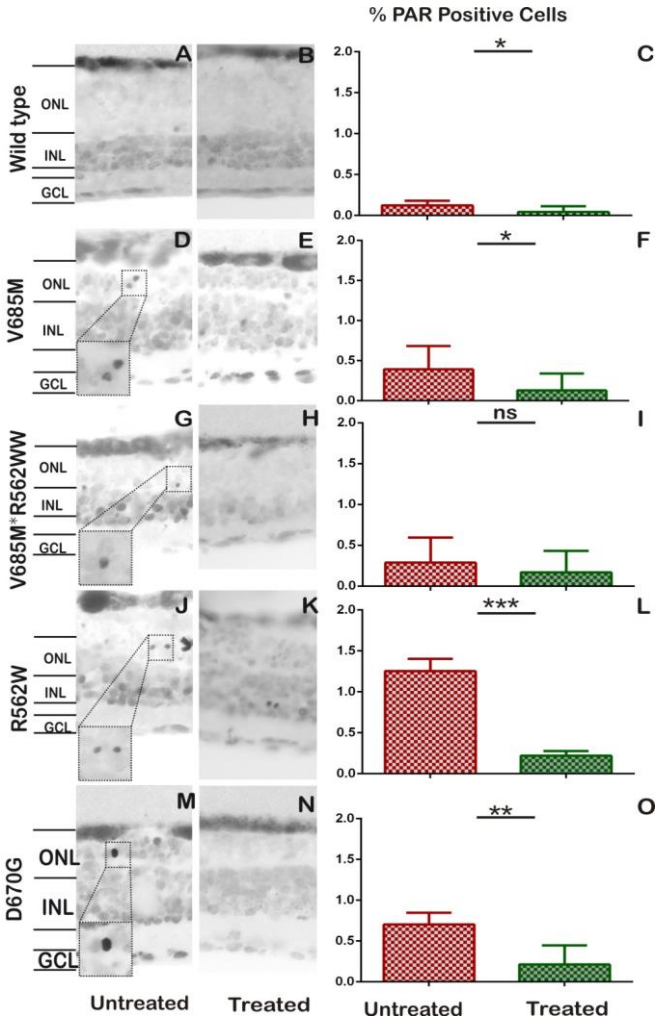

Figure 15. PARP inhibition decreases the number of PAR polymers in cells in the ONL in the different *Pde6a* mutants

PARP inhibition by PJ34 decreases the number of PAR positive cell in the $Pde6a^{V685M}$, $Pde6a^{R562W}$, $Pde6a^{V685M*R562W}$ and $Pde6a^{D670G}$ photoreceptors in short-term retinal cultures (P5–P15) (B, E, and K, N). In short-term cultures, the number of PAR positive cells in the *wt*, $Pde6a^{V685M}$, $Pde6a^{V685M*R562W}$, $Pde6a^{R562W}$ and $Pde6a^{D670G}$ ONL (A, D, E, J, M) were significant decreased by PJ34 treatment (C, F, L, O), although there was no significant difference in $Pde6a^{V685M*R562W}$ when compared with untreated specimens. The staining was representative of six specimens; *P<0.05. Scale bar represents 20 um.

3.2.4 Summary of treatment results on four Pde6a mutants in vitro

Our preliminary results from these *Pde6a* mutants indicate that treatment of PARP inhibition by PJ34 therapy can be effective, and may have large implications in the future treatment of RP patients.

Table 5.Treatment of four *Pde6a* mutants in vitro

Animal	n	TUNEL	PAR	Phot. rows
wt				
Untreated	6	1.23 ± 0.14	0.12 ± 0.02	5.89 ± 0.24
Treated		0.42 ± 0.12 (***)	0.04 ± 0.02 (*)	6.36 ± 0.44 (ns)
V685M				
Untreated	6	5.84 ± 1.08	0.39 ± 0.10	2.92 ± 0.17
Treated		1.95 ± 0.11 (*)	0.13 ± 0.06 (*)	2.33 ± 0.25 (ns)
V685M*R562W				
Untreated	6	4.11 ± 0.60	0.29 ± 0.10	2.76 ± 0.15
Treated		1.76 ± 0.11 (*)	0.17 ± 0.09 (ns)	3.50 ± 0.23 (*)
R562W				
Untreated	6	12.58 ± 2.46	1.25 ± 0.09	3.44 ± 0.22
Treated		4.63 ± 0.97 (**)	0.22 ± 0.03 (***)	5.40 ± 0.25 (**)
D670G				
Untreated	6	9.64 ± 2.69	0.70 ± 0.06	3.76 ± 0.20
Treated		2.65 ± 0.62 (**)	0.21 ± 0.10 (**)	4.69 ± 0.18 (**)

Summary of assay results between treated and untreated in the four different *Pde6a* mutants in vitro, at the post-natal day 15. TUNEL, PAR, Photoreceptor rows levels of significance were as follows: n.s.=$p>0.05$; *=$p<0.05$; **=$p<0.01$; ***=$p<0.001$. Parameters are presented as mean ± standard deviation (S.D).

4. Discussion

The development of new therapies for RP and related hereditary retinal degenerations is still hampered by a lack of understanding of the underlying pathogenic mechanisms. As it is difficult to obtain Human diseased retinal tissue, the exploration into the pathogenesis of such diseases still relies on animal models. In this study, we present one of the first studies on a compound heterozygous animal model for RP. This new animal model (*Pde6a* ^{R562W*V685M}) is exactly homologous to a human RP patient genotype and represents one of the first ever attempts to create a patient matched animal model for the development and assessment of individualized RP therapies.

4.1 Hereditary retinal degeneration and photoreceptor cell death

Inherited retinal degeneration and loss of photoreceptors may be caused by genetic mutations in a large variety of genes (Chizzolini, Galan et al. 2011). In much of the older literature apoptosis has been suggested as the key mechanism driving photoreceptor degeneration in RP (Travis 1998). However, in recent years it has become increasingly clear that in fact a variety of different neurodegenerative mechanisms are involved in photoreceptor loss (Lohr, Kuntchithapautham et al. 2006, Arango-Gonzalez, Trifunovic et al. 2014). To identify suitable targets for the development of RP therapies it is therefore important to reach a thorough understanding about the causal degenerative mechanisms (Sancho-Pelluz, Arango-Gonzalez et al. 2008). In *rd1* mouse retina a *Pde6b* mutation causes a loss of *Pde6* function and consequently a rise in intracellular cGMP, eventually leading to retinal photoreceptor cell death (Farber and Lolley 1974). High cGMP levels will result in a direct stimulation of CNG channels, allowing for an increased influx of Ca^{2+} that is thought to trigger cell death (Paquet-Durand, Beck et al. 2011). The TUNEL assay is a common method for detecting DNA fragmentation that is the end-result of cell death. In this research, TUNEL positive cell were first detected in the retinal photoreceptor cell layer of *Pde6a* mutant mice at the postnatal day 9. The number of positive cells obviously increased along with the time of retinal degeneration. A high overlap of Ca^{2+}-activated Calpain protease activity with TUNEL in *rd1* mice suggests that activation of Calpain causes cell death. However, Calpain activity may precede TUNEL,

which thus suggests that Calpain activity may be involved in earlier events during retinal photoreceptor cell death (Paquet-Durand, Johnson et al. 2007). Similarly, PARP activity is strongly elevated in *rd1* photoreceptors and PARP activity is associated with oxidative DNA damage and the nuclear translocation of apoptosis inducing factor (AIF) (Paquet-Durand, Silva et al. 2007).

These observations in the *Pde6b* mutant *rd1* mouse served as a basis for the present investigations on different *Pde6a* mutant mice. Experimental questions examined in particular are whether and how *Pde6a* gene defects lead to photoreceptor degeneration. What kind of mechanism participates in *Pde6a* mutation induced retinal degeneration, and what are the disease kinetics? In order to address these questions, in this study, we analyzed the effects of different mutations on Pde6 activity, the progression of the degeneration, and key mechanistic markers for retinal degeneration. These descriptive studies were complemented with a set of interventional experiments designed to confirm mechanistic insights and highlight new avenues for potential future RP therapy development.

4.2 Cell death mechanism in *Pde6a* mutants

Although the TUNEL assay is a method widely used for the biochemical detection of apoptosis (Gavrieli, Sherman et al. 1992), it also readily detects necrotic and other forms of cell death (Grasl-Kraupp, Ruttkay-Nedecky et al. 1995). In this research, TUNEL positive cells are detected in the retinal photoreceptor cell layer of *Pde6a* mutant mice at around 9 days after birth. As retinal degeneration progresses, there is an obvious increase in the number of TUNEL positive cells, until almost all photoreceptor cells are lost. Although the TUNEL assay clearly labels the dying cells, it is not clear what kind of cell death mechanism leads up to it. Therefore, it is still necessary to conduct additional investigations into the exact nature of the underlying cell death pathways.

Caspase is a major player in pathway of cell death. During apoptosis, PARP is cleaved and inactivated by Caspase-3, which prevents further repair of DNA damage and facilitates the execution of apoptosis (Gilliams-Francis, Quaye et al. 2003). But the broad-spectrum Caspase inhibitors are ineffective in limiting PARthanatos, which is caused by toxic accumulation of PAR in cytosol from over-activation of PARP as a unique

form of cell death (Andrabi, Dawson et al. 2008). Perhaps then Caspase does not play a substantial role during PARthanatos (Andrabi, Kim et al. 2006). This could explain why Caspase inhibitors failed to protect retinal photoreceptor cells in *rd1* and *P23H* animal models (Liu, Ge et al. 1999, Yoshizawa, Kiuchi et al. 2002). We also show this point in our experiments, where we found cells positive for cleaved and activated Caspase-3 only rarely. In fact, the numbers of Caspase-3 positive cells found in the retina of *Pde6a* mice were not significantly different from those detected in *wt* mice, indicating that in *Pde6a* animal models Caspase3 activity does not play a major role. Thus, this may be seen as additional proof that *Pde6a* mutation-induced photoreceptor cell death follows a non-apoptotic route of cell death.

Calpain, a kind of neutral cysteine protease, activated by Ca^{2+}, plays a vital role in reconstruction of the cytoskeleton, cell differentiation, apoptosis, and signal transduction (Suzuki, Hata et al. 2004). Earlier experiments showed that the activation of Calpain plays a critical role in *rd1* mouse retinal degeneration (Sancho-Pelluz, Arango-Gonzalez et al. 2008, Paquet-Durand, Sanges et al. 2010).

Calpain positive cells are detected in the retinal photoreceptor layer of animal models of all *Pde6a* mice at around P10 and their numbers were highly correlated with the progression of retinal degeneration. Calpain activity reaches its peak at P15 in ONL of *V685M*R562W* mice and *R562W* mice, at P12 in *V685M*, and at P21 in *D670G* mice. Compared to *wt* mice, it is increased significantly. This result indicates that Calpain activity may also play an important role in photoreceptor cell death in *Pde6a* mutant mice.

Table 6.Gradient of different assays in *Pde6a* mutants in vivo

TUNEL. *V685M* (P12) > *V685M*R562W* (p15) & *R562W* (P15) > *D670G* (P21)
Calpain. *V685M* (p12) > *V685M*R562W* (p15) & *R562W* (p15) > *D670G* (p21)
PARP. *V685M* (p12) > *V685M*R562W* (p13) > *R562W* (p15) > *D670G* (p21)

Altogether, there were different degrees of cell death for the four *Pde6a* mutants and a gradient from higher to lower levels of affected photoreceptors was established in the order shown above.

4.3 The role of PARP in retinal degeneration

Poly (ADP-ribose) polymerase (PARP) belongs to a group of enzymes that are involved in many different functions, including regulation of gene transcription, cell death and survival (Kraus and Hottiger 2013). Similar to Calpains, an excessive activation of PARP plays a significant role in neurodegenerative diseases (Moncada and Bolanos 2006). PARP-1 is the most well-known enzyme of the PARP family. It's mostly involved in damaged DNA repair to facilitate the repair process in both *in vivo* and *in vitro* (Dantzer, Ame et al. 2006). Furthermore, Photoreceptor cell death in several animal models including *rd1, P23H, S334ter* has been shown to be associated with excessive PARP activity (Kaur, Mencl et al. 2011). It has been suggested that PARP activation was connected to oxidative DNA damage. Furthermore, inhibition or knocking down of the PARP gene showed neuroprotection in different models for inherited retinal degeneration (Paquet-Durand, Silva et al. 2007, Sahaboglu, Tanimoto et al. 2010). This research also indicated that under normal conditions PARP activity contributes to the repair of such DNA damage. For instance, it participates in the death of retinal photoreceptor cells in a variety of rodent HRD models (Arango-Gonzalez, Trifunovic et al. 2014). However, the cell deaths that lead to photoreceptor degeneration in *Pde6a* mutants have not been well studied.

Our experiments revealed that the number of PARP positive cells in animal models of *Pde6a* mice was increased as the degeneration progressed, reaching the peak at P12 in *V685M*, at P15 in *R562W*, and at P21 in *D670G*, respectively. What's more, the TUNEL positive cells partially overlapped with the peak of PARP activation. Interestingly, PARP positive cells peaked on P13 in compound *V685M*R562W* animal models, 2 days before positive reaction in the TUNEL assay and Calpain activity. Hence, excessive activation of PARP may occur prior to retinal degenerative disease and accelerate cell death. At any rate, PARP activity clearly plays a key role in the cell death of retinal photoreceptor cells.

It is also hinted that the application of PARP inhibitors into retinal degenerative disease in the future could have a neuroprotective effect in targeted therapy.

PJ34, a kind of newly researched and developed competitive PARP inhibitor, prevents the binding of NAD^+ to the PARP enzyme, resulting in an inhibitory effect that is much stronger than previous PARP inhibitors. For example, that of traditional inhibitor-IC50 is 200nM while that of PJ34 is only 20nM. However, its enzymatic activity reaches 10.000 times of that of former (Suarez-Pinzon, Mabley et al. 2003). The molecular formula of PJ34 is C17H17N3O2. HCI, belonging to phenanthridine ketone compounds, it is water soluble, and has a high bioavailability when applied orally or intravenously. Research indicates that PJ34 plays an active role in many *in vivo* models, such as traumatic brain injury, myocardial infarction, Doxorubicin-induced myocardial failure, aging-associated heart failure, diabetic endothelial dysfunction, balloon angioplasty, endothelial injury by homocysteine, ARDS (Acute respiratory distress syndrome), hyperoxic lung injury, ovalbumin-induced asthma, mesenteric I/R injury, diabetic retinopathy and diabetic neuropathy (Garcia Soriano, Virag et al. 2001, Soriano, Pacher et al. 2001, Pacher, Cziraki et al. 2002, Pacher, Liaudet et al. 2002, Veres, Gallyas et al. 2003, Benko, Pacher et al. 2004, Jagtap, Southan et al. 2004, Zheng, Szabo et al. 2004, Casey, Black et al. 2005) while it enhances endothelium dependency of myocardium in chronic heart failure, thus remarkably reducing cell quantities of necrosis and apoptosis (Fiorillo, Ponziani et al. 2006). PJ34 also reduces photoreceptor cell death in *rd1* retinal explants (Paquet-Durand, Silva et al. 2007).

PARP could influence intracellular Ca^+ levels (Vosler, Brennan et al. 2008) through cellular pathways mediated by as of yet unknown PAR species. One pathway to cell death mediated by PARP could be through mitochondrial membrane depolarization and then open the mitochondrial permeability transition pores (MPTP) (Du, Zhang et al. 2003). Afterward, opened MPTP in turn could cause a leakage of mitochondrial proteins into the cytosol, and translocate to the nucleus (Hong, Dawson et al. 2004). Finally, it would induce peripheral chromatin condensation and DNA damage (Wang, Dawson et al. 2009). With one route, PARP transforms DNA damage and can activate DNA repair processes and induce cell death. It has been suggested PARP over activation can lead to

cell death due to neurotoxicity caused by PAR accumulation (Wang, Shimoji et al. 2003). Therefore, the application of a PARP inhibitor could prevent the cell death signal pathway. The application of PJ34 in *in vitro* organotypic retinal explant cultures derived from *Pde6a* mutant animals has a significant neuroprotective effect in retinal photoreceptor cells. However, in the very fast *V685M* animal model, there is no significant difference in retinal photoreceptor cells in treatment and non-treatment groups. The cell death of photoreceptor cells in this animal model is the fastest, reaching the peak at P13. Perhaps, at P15, when we stopped the retinal explant culturing in those animal models it was already too late. Alternatively, it would also be possible that it was linked to a stronger genetic component. However, the treatment paradigm could be optimized to start before P11 and even earlier. Also, inhibiting only a single enzyme may not be enough to sufficiently protect the photoreceptor cells, which may continue to die through other PARP-independent mechanisms. Therefore, consideration should be given to combination therapy, such as the application of Calpain and PARP inhibitors together.

4.4 Conclusion

4.4.1 Alternative cell death routes involving Calpain and PARP

In our studies, collectively, the analyzed markers (*i.e.* TUNEL, Calpain and PARP activity, PAR accumulation) coincided during their progression and followed a similar pattern in all four *Pde6a* mutants. These results have suggested that the cell death mechanisms triggered by different genetic mutations share a number of key components.

Intracellular high Ca^{2+} levels can influence the metabolism of mitochondria, causing oxidative stress, activation of PARP and Calpain. Subsequently, nuclear DNA is in turn damaged by oxidative stress, while the excessive consumption of NAD^+ and generation of PAR will have additional detrimental effects. Ca^{2+} inside the mitochondria is further imbalanced under the combined action of NAD^+ reduction and PAR accumulation; and as a consequence, the cells undergo an energy deficit. The process of maintaining apoptosis is different according to the *in vivo* positioning of mitochondria, which may be involved in multiple cell death promoting pathways. Calpain activity may promote the release of AIF, hence the elimination or inhibition of Calpain may inhibit cell death or at least delay it (Andrabi, Dawson et al. 2008, Wang, Kim et al. 2009). The high activity of Calpain

emerges in each *Pde6a* mice model and therefore, the application of Calpain inhibitors to block Calpain activity may constitute another important target for the development of retinal degeneration therapy.

Our studies identified activation of Calpain and PARP, as previously uncharacterized cell death signals in *Pde6a* mutants. Thus interfering with either Calpain or PARP may offer innovative therapeutic approaches for the treatment of cellular injury in RP.

4.4.2 PARP as a therapeutic target in Pde6a retinitis pigmentosa

Targeting critical factors of photoreceptor cell death could be a novel neuroprotective therapy in RP (Okoye, Zimmer et al. 2003). In order to test whether PARP was also responsible for photoreceptor loss caused by mutations in the *Pde6a* gene, we utilized three mouse models homozygous for the *V685M, R562W* and *D670G* mutation in *Pde6a*. Since homozygosity for mutant alleles is extremely rare in human RD patients, we also used compound heterozygous *Pde6a*$^{V685M*\mathrm{R562W}}$ animals, which were genotype matched to human RP. In all four *Pde6a* mutant situations, we found an excessive activation of PARP, which correlated in time with the progression of photoreceptor degeneration. We then used organotypic retinal explant cultures treated with the PARP specific inhibitor PJ34 to confirm the causal involvement of PARP activity in the neurodegenerative process. The neuroprotective effect of PARP inhibition was evaluated for the different genetic conditions, at different treatment time-points and durations, to establish an optimal treatment regime for later *in vivo* application. Our results highlight PARP as a target for neuroprotective interventions in RP caused by *Pde6a* mutations and are a first attempt towards personalized, genotype matched therapy development for RP.

4.4.3 Perspectives for future treatment developments

The present study uncovered the role of Calpain and PARP activity during photoreceptor degeneration in four *Pde6a* animal models, and also found that short-term retinal cultures display increased photoreceptor survival after application of the PARP inhibitor PJ34. Still, blocking only one single enzyme may not be sufficient to prevent HRD entirely, as the photoreceptor cells may be able to die through other mechanisms. Therefore, future therapy developments may need to consider using combinations of

inhibitors of Calpain proteases and PARP, and possibly even further cellular targets involved in HRD.

5. Zusammenfassung

Ziel. Retinitis Pigmentosa (RP) ist eine Gruppe heterogener Krankheiten, die zu Erblindung führt und in der Summe mit einer Häufigkeit von 1 in 4000 Individuen weltweit auftritt. RP ist gekennzeichnet durch eine hohe genetische Diversität, bei der Mutationen desselben Gens zu sehr verschiedenen Phänotypen führen können. Bisher lag der Fokus der Forschung auf Mutationen in *Pde6b* (Keeler 1924, Chang, Hawes et al. 2002), während *Pde6a* Mutationen weit weniger untersucht wurden, obwohl sie ebenfalls zu Zelltod der Photorezeptor-Stäbchen führen und RP verursachen.

Methoden. Die Experimente der vorliegenden Arbeit wurden in zwei Schritten durchgeführt: im ersten die Charakterisierung der retinalen Degeneration ***in vivo*** und im zweiten die ***in vitro*** Behandlung von Gewebe von *Pde6a* Mutanten. Für die Charakterisierung der retinalen Degeneration ***in vivo*** haben wir vier unterschiedliche homozygote *Pde6a* Mauslinien verwendet, und zwar $Pde6a^{V685M}$, $Pde6a^{D670G}$, $Pde6a^{R562W}$ und $Pde6a^{V685M*R562W}$. Wir haben in den *Pde6a* Mauslinien mit den folgenden Markern den Fortschritt der Degeneration der Photorezeptoren beschrieben: - TUNEL-Signal, - Caspase-3, - Calpain-Aktivität, - PARP-Aktivität und - PAR-Polymere. 2) Für eine Charakterisierung der Wirkung der Inhibition von PARP ***in vitro*** haben wir organotypische Kulturen von Retinas der verschiedenen Mauslinien verwendet. Diese Kulturen wurden mit dem pharmakologischen PARP Inhibitor PJ34 behandelt, um zu bestätitigen, dass PARP-Aktivität eine Ursache des neurodegenerativen Prozesses ist.

Ergebnisse. Unsere Untersuchung zeigt auf, dass das Tempo der retinalen Degeneration in vivo in den vier *Pde6a* Mutationen unterschiedlich ist und dass der Verlauf der Degeneration der Photorezeptoren immer korreliert ist mit erhöhten Signalen bei der Messung von TUNEL, PARP-Aktivität, PARylierten Proteinen und Calpain-Aktivität. Die Aktivität von Caspase-3 zeigte keine Erhöhung bei der retinalen Degeneration der *Pde6a* Mutanten. Der Einsatz eines pharmakologischen Inhibitors von PARP in organotypische Kulturen von Retinas von *Pde6a* Mäusen bestätigte, dass PARP eine Rolle spielt in der retinalen Degeneration von Mäusen der vier Genotypen. Die neuroprotektive Wirkung des PARP Inhibitors wurde in den vier Genotypen zu verschiedenen Zeitpunkten und für verschiedene Expositionszeiten nachgewiesen.

Ausblick. Wir konnten zeigen, dass die Enzyme Calpain und PARP im Verlauf der Degeneration der Photorezeptoren in verschiedenen *Pde6a* Mutanten eine zentrale Rolle spielen. Unsere Untersuchung unterstreicht, dass das PARP Enzym ein gemeinsames pharmakologisches Ziel sein kann für neuroprotektive Massnahmen in jenen Fällen der RP, denen *Pde6a* Mutationen zugrunde liegen. Darüber hinaus kann die vorliegende Studie dazu dienen, den Zeitverlauf der retinalen Degeneration bei RP Patienten vorherzusagen, deren RP unterschiedliche *Pde6a* Mutationen zugrunde liegen, und die Studie kann helfen, den optimalen Zeitpunkt für klinische Intervention festzulegen.

6. Publication or Presentations

Publications.

Vithiyanjali Sothilingam [1§], Marina Garcia-Garrido [1§], ***Kangwei Jiao [2§],*** *Elena Buena-Atienza [3], Ayse Sahaboglu [2], Dragana Trifunović [2], Sukirthini Balendran [3†], Tanja Grau Koepfli [3*], Susanne C. Beck [1], Christian Schön [4], Martin Biel [4], Angelique Heckmann [5], Regine Mühlfriedel [1], Stylianos Michalakis [4], Bernd Wissinger [3#], Mathias W. Seeliger [1#], François Paquet-Durand [2#]* Retinitis Pigmentosa: Impact of different Pde6a point mutations on the disease phenotype. Hum Mol Genet. 2015 Jul 17. pii: ddv275.

Kangwei Jiao [1,2#] , Ayse Sahaboglu [1#§], Eberhart Zrenner [3,4], Marius Ueffing [4], Per A. R. Ekström [5], François Paquet-Durand [1§], Efficacy of PARP inhibition in Pde6a mutant mouse models for retinitis pigmentosa depends on the quality and composition of individual human mutations. Molecular Neurodegeneration. (Manuscript under review).

Oral Presentations.

Jiao KW*, Sahaboglu A, van Veen T, Zrenner E, Marius Ueffing, Paquet-Durand F.* (2014) Mechanism of photoreceptor cell death in *Pde6a* mutants Progress report, Seminar, Tübingen University, Germany, Oct 15.

Jiao KW*, Sahaboglu A, van Veen T, Zrenner E, Marius Ueffing, Paquet-Durand F*. (2015) Evaluation of neuroprotective interventions in different *Pde6a* mutant animal models for Retinitis Pigmentosa**.** Progress report,Seminar, Tübingen University, Germany, May 13.

Posters.

Kangwei Jiao [1,3#], *Ayse Sahaboglu [1#], Nicole Weisschuh [2], Per Ekstrom[2], Marius Ueffing[1], François Paquet-Durand [1]* Pro-Retina Meeting 2015, Potsdam, Berlin, Germany (Poster presented)

7. Curriculum Vitae

Education Background:

Eberhard-Karls-University of Tübingen, Germany

Centre for Ophthalmology, Institute for Ophthalmic Research,

Cell death mechanisms group,

October, 2013- Present: Dr. Med

Wuhan University, China

Faculty of Medical

Ophthalmology

September, 2010- July, 2013: Master

Professional Experience

2nd Hospital of Yunnan Province & 4th Affiliated Hospital Of Kunming Medical University

June 2013- Present: Senior Resident

Center for Ophthalmology, Kunming Tongren Hospital

Oct. 2006-Jun. 2010: Senior Resident

Center for Ophthalmology, Beijing Tongren Hospital & Capital Medical University

Jun. 2004-Oct. 2006: Resident

8. Acknowledgements

My doctoral dissertation could not have been written without the support of many wonderful people.

At the top of my list,

I must thank

Dr. François Paquet-Durand, my supervisor, who is responsible for all things in our group. He is fantastic at his job, and is priceless when it comes to making my dissertation, papers, and manuscripts as good as they can possibly be, even during his very busy schedule.

Dr. Ayse Sahaboglu-Tekgöz, also one of my supervisors. It was hard for me to adapt, especially at first, to new circumstances as a foreigner who had never put his foot on foreign soil, and working with her has made me one of the luckiest students around.

I must also thank **Prof. Dr. Marius Ueffing**, I am grateful for his encouragement and constant support for my work and to **Prof. Dr. Bernd Wissinger** for giving me so many valuable comment suggestions during the Potsdam meeting in Berlin.

My thanks also go to **Dr. Matthias Gerberding**, who does so much for me in yet another complex and critically important area of my life and work.

Fellow **PhD student Manoj Kulkarni**, close as a brother, also deserves my heartfelt thanks not only for being the best friend a guy can have, but for all the effort, hard work, and my every stupid question that was solved by him.

My thanks also go out to both **Melanie Barth and Joaquin Valdes Bize**, who are always there to answer my questions, and I'd like to extend a special thanks to **Joaquin Valdes Bize**, for his painstaking review of this thesis.

Dr. Daniel Rathbun and **Dr. Megan Rathbun**, native English speakers, also deserve my thanks for helping to polish this thesis as smooth as possible.

Also to **Dr. Blanca Arango-Gonzalez**, who was my supervisor in the very begining. She deserves my thanks not only for all she does, but also because I consider her a cherished friend.

Dr. Dragana Trifunović, a very nice adviser, I am grateful to her for her helpful suggestions.

I would be remiss if I didn't thank **Norman Rieger** and **Klaudija Masarini**, who help to arrange all animals and laboratory equipment that I needed, even on weekends.

Most importantly, none of this would have been possible without the love and patience of my family that has been a constant source of love, concern, support and strength all these years. Time is really valuable for everyone, here, I would like to extend an expression of my heart-felt gratitude to my wife, **Junyu Liu**, who sacrificed her valuable time to accompany me all this way and it has been a joy to share with her "*the most wonderful and longest ride*" of our lives.

9. Bibliography

Andrabi, S. A., T. M. Dawson and V. L. Dawson (2008). "Mitochondrial and nuclear cross talk in cell death: parthanatos." Ann N Y Acad Sci **1147**: 233-241.

Andrabi, S. A., N. S. Kim, S. W. Yu, H. Wang, D. W. Koh, M. Sasaki, J. A. Klaus, T. Otsuka, Z. Zhang, R. C. Koehler, P. D. Hurn, G. G. Poirier, V. L. Dawson and T. M. Dawson (2006). "Poly(ADP-ribose) (PAR) polymer is a death signal." Proc Natl Acad Sci U S A **103**(48): 18308-18313.

Aramant, R. B. and M. J. Seiler (2004). "Progress in retinal sheet transplantation." Prog Retin Eye Res **23**(5): 475-494.

Arango-Gonzalez, B., D. Trifunovic, A. Sahaboglu, K. Kranz, S. Michalakis, P. Farinelli, S. Koch, F. Koch, S. Cottet, U. Janssen-Bienhold, K. Dedek, M. Biel, E. Zrenner, T. Euler, P. Ekstrom, M. Ueffing and F. Paquet-Durand (2014). "Identification of a common non-apoptotic cell death mechanism in hereditary retinal degeneration." PLoS One **9**(11): e112142.

Azarian, S. M., C. L. Schlamp and D. S. Williams (1993). "Characterization of calpain II in the retina and photoreceptor outer segments." J Cell Sci **105 (Pt 3)**: 787-798.

Azuma, M., K. Sakamoto-Mizutani, T. Nakajima, S. Kanaami-Daibo, Y. Tamada and T. R. Shearer (2004). "Involvement of calpain isoforms in retinal degeneration in WBN/Kob rats." Comp Med **54**(5): 533-542.

Bayes, M., M. Giordano, S. Balcells, D. Grinberg, L. Vilageliu, I. Martinez, C. Ayuso, J. Benitez, M. A. Ramos-Arroyo, P. Chivelet and et al. (1995). "Homozygous tandem duplication within the gene encoding the beta-subunit of rod phosphodiesterase as a cause for autosomal recessive retinitis pigmentosa." Hum Mutat **5**(3): 228-234.

Benko, R., P. Pacher, A. Vaslin, M. Kollai and C. Szabo (2004). "Restoration of the endothelial function in the aortic rings of apolipoprotein E deficient mice by pharmacological inhibition of the nuclear enzyme poly(ADP-ribose) polymerase." Life Sci **75**(10): 1255-1261.

Bennett, J., Y. Zeng, R. Bajwa, L. Klatt, Y. Li and A. M. Maguire (1998). "Adenovirus-mediated delivery of rhodopsin-promoted bcl-2 results in a delay in photoreceptor cell death in the rd/rd mouse." Gene Ther **5**(9): 1156-1164.

Berger, N. A., J. L. Sims, D. M. Catino and S. J. Berger (1983). "Poly(ADP-ribose) polymerase mediates the suicide response to massive DNA damage: studies in normal and DNA-repair defective cells." Princess Takamatsu Symp **13**: 219-226.

Boehmerle, W. and M. Endres (2011). "Salinomycin induces calpain and cytochrome c-mediated neuronal cell death." Cell Death Dis **2**: e168.

Casao, A., M. Mata-Campuzano, L. Ordas, J. A. Cebrian-Perez, T. Muino-Blanco and F. Martinez-Pastor (2015). "Cleaved PARP-1, an Apoptotic Marker, can be Detected in Ram Spermatozoa." Reprod Domest Anim.

Casey, P. J., J. H. Black, C. Szabo, M. Frosch, H. Albadawi, M. Chen, R. P. Cambria and M. T. Watkins (2005). "Poly(adenosine diphosphate ribose) polymerase inhibition modulates spinal cord dysfunction after thoracoabdominal aortic ischemia-reperfusion." J Vasc Surg **41**(1): 99-107.

Chang, B., N. L. Hawes, R. E. Hurd, M. T. Davisson, S. Nusinowitz and J. R. Heckenlively (2002). "Retinal degeneration mutants in the mouse." Vision Res **42**(4): 517-525.

Chen, Q., M. Paillard, L. Gomez, T. Ross, Y. Hu, A. Xu and E. J. Lesnefsky (2011). "Activation of mitochondrial mu-calpain increases AIF cleavage in cardiac mitochondria during ischemia-reperfusion." Biochem Biophys Res Commun **415**(4): 533-538.

Chizzolini, M., A. Galan, E. Milan, A. Sebastiani, C. Costagliola and F. Parmeggiani (2011). "Good epidemiologic practice in retinitis pigmentosa: from phenotyping to biobanking." Curr Genomics **12**(4): 260-266.

Dantzer, F., J. C. Ame, V. Schreiber, J. Nakamura, J. Menissier-de Murcia and G. de Murcia (2006). "Poly(ADP-ribose) polymerase-1 activation during DNA damage and repair." Methods Enzymol **409**: 493-510.

Dayton, W. R., D. E. Goll, M. G. Zeece, R. M. Robson and W. J. Reville (1976). "A Ca2+-activated protease possibly involved in myofibrillar protein turnover. Purification from porcine muscle." Biochemistry **15**(10): 2150-2158.

Delyfer, M. N., T. Leveillard, S. Mohand-Said, D. Hicks, S. Picaud and J. A. Sahel (2004). "Inherited retinal degenerations: therapeutic prospects." Biol Cell **96**(4): 261-269.

Donovan, M. and T. G. Cotter (2002). "Caspase-independent photoreceptor apoptosis in vivo and differential expression of apoptotic protease activating factor-1 and caspase-3 during retinal development." Cell Death Differ **9**(11): 1220-1231.

Doonan, F., M. Donovan and T. G. Cotter (2003). "Caspase-independent photoreceptor apoptosis in mouse models of retinal degeneration." J Neurosci **23**(13): 5723-5731.

Dryja, T. P., D. E. Rucinski, S. H. Chen and E. L. Berson (1999). "Frequency of mutations in the gene encoding the alpha subunit of rod cGMP-phosphodiesterase in autosomal recessive retinitis pigmentosa." Invest Ophthalmol Vis Sci **40**(8): 1859-1865.

Du, L., X. Zhang, Y. Y. Han, N. A. Burke, P. M. Kochanek, S. C. Watkins, S. H. Graham, J. A. Carcillo, C. Szabo and R. S. Clark (2003). "Intra-mitochondrial poly(ADP-ribosylation) contributes to NAD+ depletion and cell death induced by oxidative stress." J Biol Chem **278**(20): 18426-18433.

Farber, D. B. and R. N. Lolley (1974). "Cyclic guanosine monophosphate: elevation in degenerating photoreceptor cells of the C3H mouse retina." Science **186**(4162): 449-451.

Fariss, R. N., Z. Y. Li and A. H. Milam (2000). "Abnormalities in rod photoreceptors, amacrine cells, and horizontal cells in human retinas with retinitis pigmentosa." Am J Ophthalmol **129**(2): 215-223.

Fesenko, E. E., S. S. Kolesnikov and A. L. Lyubarsky (1985). "Induction by cyclic GMP of cationic conductance in plasma membrane of retinal rod outer segment." Nature **313**(6000): 310-313.

Fiorillo, C., V. Ponziani, L. Giannini, C. Cecchi, A. Celli, N. Nassi, L. Lanzilao, R. Caporale and P. Nassi (2006). "Protective effects of the PARP-1 inhibitor PJ34 in hypoxic-reoxygenated cardiomyoblasts." Cell Mol Life Sci **63**(24): 3061-3071.

Garcia Soriano, F., L. Virag, P. Jagtap, E. Szabo, J. G. Mabley, L. Liaudet, A. Marton, D. G. Hoyt, K. G. Murthy, A. L. Salzman, G. J. Southan and C. Szabo (2001). "Diabetic endothelial dysfunction: the role of poly(ADP-ribose) polymerase activation." Nat Med **7**(1): 108-113.

Gavrieli, Y., Y. Sherman and S. A. Ben-Sasson (1992). "Identification of programmed cell death in situ via specific labeling of nuclear DNA fragmentation." J Cell Biol **119**(3): 493-501.

Gilliams-Francis, K. L., A. A. Quaye and J. R. Naegele (2003). "PARP cleavage, DNA fragmentation, and pyknosis during excitotoxin-induced neuronal death." Exp Neurol **184**(1): 359-372.

Grasl-Kraupp, B., B. Ruttkay-Nedecky, H. Koudelka, K. Bukowska, W. Bursch and R. Schulte-Hermann (1995). "In situ detection of fragmented DNA (TUNEL assay) fails to discriminate among apoptosis, necrosis, and autolytic cell death: a cautionary note." Hepatology **21**(5): 1465-1468.

Gressner, A. M., B. Lahme and S. Roth (1997). "Attenuation of TGF-beta-induced apoptosis in primary cultures of hepatocytes by calpain inhibitors." Biochem Biophys Res Commun **231**(2): 457-462.

Guroff, G. (1964). "A Neutral, Calcium-Activated Proteinase from the Soluble Fraction of Rat Brain." J Biol Chem **239**: 149-155.

Hartong, D. T., E. L. Berson and T. P. Dryja (2006). "Retinitis pigmentosa." Lancet **368**(9549): 1795-1809.

Herceg, Z. and Z. Q. Wang (2001). "Functions of poly(ADP-ribose) polymerase (PARP) in DNA repair, genomic integrity and cell death." Mutat Res **477**(1-2): 97-110.

Hong, S. J., T. M. Dawson and V. L. Dawson (2004). "Nuclear and mitochondrial conversations in cell death: PARP-1 and AIF signaling." Trends Pharmacol Sci **25**(5): 259-264.

Hood, J. L., W. H. Brooks and T. L. Roszman (2006). "Subcellular mobility of the calpain/calpastatin network: an organelle transient." Bioessays **28**(8): 850-859.

Huang, Y. and K. K. Wang (2001). "The calpain family and human disease." Trends Mol Med **7**(8): 355-362.

Inoue, Y., A. Iriyama, S. Ueno, H. Takahashi, M. Kondo, Y. Tamaki, M. Araie and Y. Yanagi (2007). "Subretinal transplantation of bone marrow mesenchymal stem cells delays retinal degeneration in the RCS rat model of retinal degeneration." Exp Eye Res **85**(2): 234-241.

Ishiura, S., H. Murofushi, K. Suzuki and K. Imahori (1978). "Studies of a calcium-activated neutral protease from chicken skeletal muscle. I. Purification and characterization." J Biochem **84**(1): 225-230.

Jagtap, P. G., G. J. Southan, E. Baloglu, S. Ram, J. G. Mabley, A. Marton, A. Salzman and C. Szabo (2004). "The discovery and synthesis of novel adenosine substituted 2,3-dihydro-1H-isoindol-1-ones: potent inhibitors of poly(ADP-ribose) polymerase-1 (PARP-1)." Bioorg Med Chem Lett **14**(1): 81-85.

Kar, P., T. Chakraborti, K. Samanta and S. Chakraborti (2009). "mu-Calpain mediated cleavage of the Na+/Ca2+ exchanger in isolated mitochondria under A23187 induced Ca2+ stimulation." Arch Biochem Biophys **482**(1-2): 66-76.

Kar, P., K. Samanta, S. Shaikh, A. Chowdhury, T. Chakraborti and S. Chakraborti (2010). "Mitochondrial calpain system: an overview." Arch Biochem Biophys **495**(1): 1-7.

Kaur, J., S. Mencl, A. Sahaboglu, P. Farinelli, T. van Veen, E. Zrenner, P. Ekstrom, F. Paquet-Durand and B. Arango-Gonzalez (2011). "Calpain and PARP activation during photoreceptor cell death in P23H and S334ter rhodopsin mutant rats." PLoS One **6**(7): e22181.

Keeler, C. E. (1924). "The Inheritance of a Retinal Abnormality in White Mice." Proc Natl Acad Sci U S A **10**(7): 329-333.

Kerr, J. F., A. H. Wyllie and A. R. Currie (1972). "Apoptosis: a basic biological phenomenon with wide-ranging implications in tissue kinetics." Br J Cancer **26**(4): 239-257.

Kishimoto, A., N. Kajikawa, H. Tabuchi, M. Shiota and Y. Nishizuka (1981). "Calcium-dependent neural proteases, widespread occurrence of a species of protease active at lower concentrations of calcium." J Biochem **90**(3): 889-892.

Komeima, K., B. S. Rogers and P. A. Campochiaro (2007). "Antioxidants slow photoreceptor cell death in mouse models of retinitis pigmentosa." J Cell Physiol **213**(3): 809-815.

Koutalos, Y., K. Nakatani and K. W. Yau (1995). "The cGMP-phosphodiesterase and its contribution to sensitivity regulation in retinal rods." J Gen Physiol **106**(5): 891-921.

Kraus, W. L. and M. O. Hottiger (2013). "PARP-1 and gene regulation: progress and puzzles." Mol Aspects Med **34**(6): 1109-1123.

Langelier, M. F., J. L. Planck, S. Roy and J. M. Pascal (2012). "Structural basis for DNA damage-dependent poly(ADP-ribosyl)ation by human PARP-1." Science **336**(6082): 728-732.

Lavail, M. M., L. Li, J. E. Turner and D. Yasumura (1992). "Retinal pigment epithelial cell transplantation in RCS rats: normal metabolism in rescued photoreceptors." Exp Eye Res **55**(4): 555-562.

Leist, M. and M. Jaattela (2001). "Four deaths and a funeral: from caspases to alternative mechanisms." Nat Rev Mol Cell Biol **2**(8): 589-598.

Liang, F. Q., G. Allen and D. Earnest (2000). "Role of brain-derived neurotrophic factor in the circadian regulation of the suprachiasmatic pacemaker by light." J Neurosci **20**(8): 2978-2987.

Liebman, P. A. (1987). "Visual receptor transduction." Ann N Y Acad Sci **494**: 65-74.

Liu, H., J. Ge, Y. Guo and Z. Yang (1999). "The study of influencing factors on the growth characters of Sprague-Dawley rat retinal neurons in vitro." Yan Ke Xue Bao **15**(3): 141-145.

Lohr, H. R., K. Kuntchithapautham, A. K. Sharma and B. Rohrer (2006). "Multiple, parallel cellular suicide mechanisms participate in photoreceptor cell death." Exp Eye Res **83**(2): 380-389.

Loo, D. T. (2002). "TUNEL assay. An overview of techniques." Methods Mol Biol **203**: 21-30.

Malanga, M. and F. R. Althaus (2005). "The role of poly(ADP-ribose) in the DNA damage signaling network." Biochem Cell Biol **83**(3): 354-364.

Marc, R. E., B. W. Jones, J. R. Anderson, K. Kinard, D. W. Marshak, J. H. Wilson, T. Wensel and R. J. Lucas (2007). "Neural reprogramming in retinal degeneration." Invest Ophthalmol Vis Sci **48**(7): 3364-3371.

Marek, L. (2013). "[The role of the apoptosome in the activation of procaspase-9]." Postepy Hig Med Dosw (Online) **67**: 54-64.

Martinez, J. A., Z. Zhang, S. I. Svetlov, R. L. Hayes, K. K. Wang and S. F. Larner (2010). "Calpain and caspase processing of caspase-12 contribute to the ER stress-induced cell death pathway in differentiated PC12 cells." Apoptosis **15**(12): 1480-1493.

McConkey, D. J., P. Nicotera, P. Hartzell, G. Bellomo, A. H. Wyllie and S. Orrenius (1989). "Glucocorticoids activate a suicide process in thymocytes through an elevation of cytosolic Ca2+ concentration." Arch Biochem Biophys **269**(1): 365-370.

Mohand-Said, S., D. Hicks, H. Dreyfus and J. A. Sahel (2000). "Selective transplantation of rods delays cone loss in a retinitis pigmentosa model." Arch Ophthalmol **118**(6): 807-811.

Moncada, S. and J. P. Bolanos (2006). "Nitric oxide, cell bioenergetics and neurodegeneration." J Neurochem **97**(6): 1676-1689.

Nelson, W. B., A. J. Smuder, M. B. Hudson, E. E. Talbert and S. K. Powers (2012). "Cross-talk between the calpain and caspase-3 proteolytic systems in the diaphragm during prolonged mechanical ventilation." Crit Care Med **40**(6): 1857-1863.

Norberg, E., S. Orrenius and B. Zhivotovsky (2010). "Mitochondrial regulation of cell death: processing of apoptosis-inducing factor (AIF)." Biochem Biophys Res Commun **396**(1): 95-100.

Ohno, S., Y. Emori, S. Imajoh, H. Kawasaki, M. Kisaragi and K. Suzuki (1984). "Evolutionary origin of a calcium-dependent protease by fusion of genes for a thiol protease and a calcium-binding protein?" Nature **312**(5994): 566-570.

Okoye, G., J. Zimmer, J. Sung, P. Gehlbach, T. Deering, H. Nambu, S. Hackett, M. Melia, N. Esumi, D. J. Zack and P. A. Campochiaro (2003). "Increased expression of brain-derived neurotrophic factor preserves retinal function and slows cell death from rhodopsin mutation or oxidative damage." J Neurosci **23**(10): 4164-4172.

Pacher, P., A. Cziraki, J. G. Mabley, L. Liaudet, L. Papp and C. Szabo (2002). "Role of poly(ADP-ribose) polymerase activation in endotoxin-induced cardiac collapse in rodents." Biochem Pharmacol **64**(12): 1785-1791.

Pacher, P., L. Liaudet, P. Bai, L. Virag, J. G. Mabley, G. Hasko and C. Szabo (2002). "Activation of poly(ADP-ribose) polymerase contributes to development of doxorubicin-induced heart failure." J Pharmacol Exp Ther **300**(3): 862-867.

Papermaster, D. S. and J. Windle (1995). "Death at an early age. Apoptosis in inherited retinal degenerations." Invest Ophthalmol Vis Sci **36**(6): 977-983.

Paquet-Durand, F., S. Azadi, S. M. Hauck, M. Ueffing, T. van Veen and P. Ekstrom (2006). "Calpain is activated in degenerating photoreceptors in the rd1 mouse." J Neurochem **96**(3): 802-814.

Paquet-Durand, F., S. Beck, S. Michalakis, T. Goldmann, G. Huber, R. Muhlfriedel, D. Trifunovic, M. D. Fischer, E. Fahl, G. Duetsch, E. Becirovic, U. Wolfrum, T. van Veen, M. Biel, N. Tanimoto and M. W. Seeliger (2011). "A key role for cyclic nucleotide gated (CNG) channels in cGMP-related retinitis pigmentosa." Hum Mol Genet **20**(5): 941-947.

Paquet-Durand, F., L. Johnson and P. Ekstrom (2007). "Calpain activity in retinal degeneration." J Neurosci Res **85**(4): 693-702.

Paquet-Durand, F., D. Sanges, J. McCall, J. Silva, T. van Veen, V. Marigo and P. Ekstrom (2010). "Photoreceptor rescue and toxicity induced by different calpain inhibitors." J Neurochem **115**(4): 930-940.

Paquet-Durand, F., J. Silva, T. Talukdar, L. E. Johnson, S. Azadi, T. van Veen, M. Ueffing, S. M. Hauck and P. A. Ekstrom (2007). "Excessive activation of poly(ADP-ribose) polymerase contributes to inherited photoreceptor degeneration in the retinal degeneration 1 mouse." J Neurosci **27**(38): 10311-10319.

Petrucco, S. and R. Percudani (2008). "Structural recognition of DNA by poly(ADP-ribose)polymerase-like zinc finger families." FEBS J **275**(5): 883-893.

Sahaboglu, A., N. Tanimoto, J. Kaur, J. Sancho-Pelluz, G. Huber, E. Fahl, B. Arango-Gonzalez, E. Zrenner, P. Ekstrom, H. Lowenheim, M. Seeliger and F. Paquet-Durand (2010). "PARP1 gene knock-out increases resistance to retinal degeneration without affecting retinal function." PLoS One **5**(11): e15495.

Saito, K., J. S. Elce, J. E. Hamos and R. A. Nixon (1993). "Widespread activation of calcium-activated neutral proteinase (calpain) in the brain in Alzheimer disease: a potential molecular basis for neuronal degeneration." Proc Natl Acad Sci U S A **90**(7): 2628-2632.

Sakamoto, K., M. McCluskey, T. G. Wensel, J. K. Naggert and P. M. Nishina (2009). "New mouse models for recessive retinitis pigmentosa caused by mutations in the Pde6a gene." Hum Mol Genet **18**(1): 178-192.

Sancho-Pelluz, J., B. Arango-Gonzalez, S. Kustermann, F. J. Romero, T. van Veen, E. Zrenner, P. Ekstrom and F. Paquet-Durand (2008). "Photoreceptor cell death mechanisms in inherited retinal degeneration." Mol Neurobiol **38**(3): 253-269.

Schmitz, Y. and P. Witkovsky (1997). "Dependence of photoreceptor glutamate release on a dihydropyridine-sensitive calcium channel." Neuroscience **78**(4): 1209-1216.

Silverman, M. S. and S. E. Hughes (1990). "Photoreceptor rescue in the RCS rat without pigment epithelium transplantation." Curr Eye Res **9**(2): 183-191.

Sims, J. L., S. J. Berger and N. A. Berger (1983). "Poly(ADP-ribose) Polymerase inhibitors preserve nicotinamide adenine dinucleotide and adenosine 5'-triphosphate pools in DNA-damaged cells: mechanism of stimulation of unscheduled DNA synthesis." Biochemistry **22**(22): 5188-5194.

Soriano, F. G., P. Pacher, J. Mabley, L. Liaudet and C. Szabo (2001). "Rapid reversal of the diabetic endothelial dysfunction by pharmacological inhibition of poly(ADP-ribose) polymerase." Circ Res **89**(8): 684-691.

Suarez-Pinzon, W. L., J. G. Mabley, R. Power, C. Szabo and A. Rabinovitch (2003). "Poly (ADP-ribose) polymerase inhibition prevents spontaneous and recurrent autoimmune diabetes in NOD mice by inducing apoptosis of islet-infiltrating leukocytes." Diabetes **52**(7): 1683-1688.

Suzuki, K., S. Hata, Y. Kawabata and H. Sorimachi (2004). "Structure, activation, and biology of calpain." Diabetes **53 Suppl 1**: S12-18.

Swindall, A. F., J. A. Stanley and E. S. Yang (2013). "PARP-1: Friend or Foe of DNA Damage and Repair in Tumorigenesis?" Cancers (Basel) **5**(3): 943-958.

Szel, A. and P. Rohlich (1992). "Two cone types of rat retina detected by anti-visual pigment antibodies." Exp Eye Res **55**(1): 47-52.

Travis, G. H. (1998). "Mechanisms of cell death in the inherited retinal degenerations." Am J Hum Genet **62**(3): 503-508.

Trifunovic, D., A. Sahaboglu, J. Kaur, S. Mencl, E. Zrenner, M. Ueffing, B. Arango-Gonzalez and F. Paquet-Durand (2012). "Neuroprotective strategies for the treatment of inherited photoreceptor degeneration." Curr Mol Med **12**(5): 598-612.

Tsang, S. H., P. Gouras, C. K. Yamashita, H. Kjeldbye, J. Fisher, D. B. Farber and S. P. Goff (1996). "Retinal degeneration in mice lacking the gamma subunit of the rod cGMP phosphodiesterase." Science **272**(5264): 1026-1029.

Uteza, Y., J. S. Rouillot, A. Kobetz, D. Marchant, S. Pecqueur, E. Arnaud, H. Prats, J. Honiger, J. L. Dufier, M. Abitbol and M. Neuner-Jehle (1999). "Intravitreous transplantation of encapsulated fibroblasts secreting the human fibroblast growth factor 2 delays photoreceptor cell degeneration in Royal College of Surgeons rats." Proc Natl Acad Sci U S A **96**(6): 3126-3131.

Veres, B., F. Gallyas, Jr., G. Varbiro, Z. Berente, E. Osz, G. Szekeres, C. Szabo and B. Sumegi (2003). "Decrease of the inflammatory response and induction of the Akt/protein kinase B pathway by poly-(ADP-ribose) polymerase 1 inhibitor in endotoxin-induced septic shock." Biochem Pharmacol **65**(8): 1373-1382.

Vosler, P. S., C. S. Brennan and J. Chen (2008). "Calpain-mediated signaling mechanisms in neuronal injury and neurodegeneration." Mol Neurobiol **38**(1): 78-100.

Vosler, P. S., D. Sun, S. Wang, Y. Gao, D. B. Kintner, A. P. Signore, G. Cao and J. Chen (2009). "Calcium dysregulation induces apoptosis-inducing factor release: cross-talk between PARP-1- and calpain-signaling pathways." Exp Neurol **218**(2): 213-220.

Wang, H., M. Shimoji, S. W. Yu, T. M. Dawson and V. L. Dawson (2003). "Apoptosis inducing factor and PARP-mediated injury in the MPTP mouse model of Parkinson's disease." Ann N Y Acad Sci **991**: 132-139.

Wang, Y., V. L. Dawson and T. M. Dawson (2009). "Poly(ADP-ribose) signals to mitochondrial AIF: a key event in parthanatos." Exp Neurol **218**(2): 193-202.

Wang, Y., N. S. Kim, X. Li, P. A. Greer, R. C. Koehler, V. L. Dawson and T. M. Dawson (2009). "Calpain activation is not required for AIF translocation in PARP-1-dependent cell death (parthanatos)." J Neurochem **110**(2): 687-696.

Ying, S., H. T. Jansen, M. N. Lehman, S. L. Fong and W. W. Kao (2000). "Retinal degeneration in cone photoreceptor cell-ablated transgenic mice." Mol Vis **6**: 101-108.

Yoshizawa, K., K. Kiuchi, H. Nambu, J. Yang, H. Senzaki, Y. Kiyozuka, N. Shikata and A. Tsubura (2002). "Caspase-3 inhibitor transiently delays inherited retinal degeneration in C3H mice carrying the rd gene." Graefes Arch Clin Exp Ophthalmol **240**(3): 214-219.

Yu, D. Y. and S. J. Cringle (2005). "Retinal degeneration and local oxygen metabolism." Exp Eye Res **80**(6): 745-751.

Yu, Z., T. Kuncewicz, W. P. Dubinsky and B. C. Kone (2006). "Nitric oxide-dependent negative feedback of PARP-1 trans-activation of the inducible nitric-oxide synthase gene." J Biol Chem **281**(14): 9101-9109.

Zheng, L., C. Szabo and T. S. Kern (2004). "Poly(ADP-ribose) polymerase is involved in the development of diabetic retinopathy via regulation of nuclear factor-kappaB." Diabetes **53**(11): 2960-2967.

Statement of Authorship

I hereby declare that I have produced the work entitled: *"Evaluation of neuroprotective interventions in different Pde6a mutant animal models for Retinitis Pigmentosa"* submitted for the award of a doctorate, on my own (without external help), have used only the sources and aids indicated, and have marked passages included from other works, whether verbatim or in context, as such.

I swear under oath that these statements are true and that I have not concealed anything. I am aware that making a false declaration under oath is punishable by a term of imprisonment of up to three years or by a fine.

Kangwei JIAO